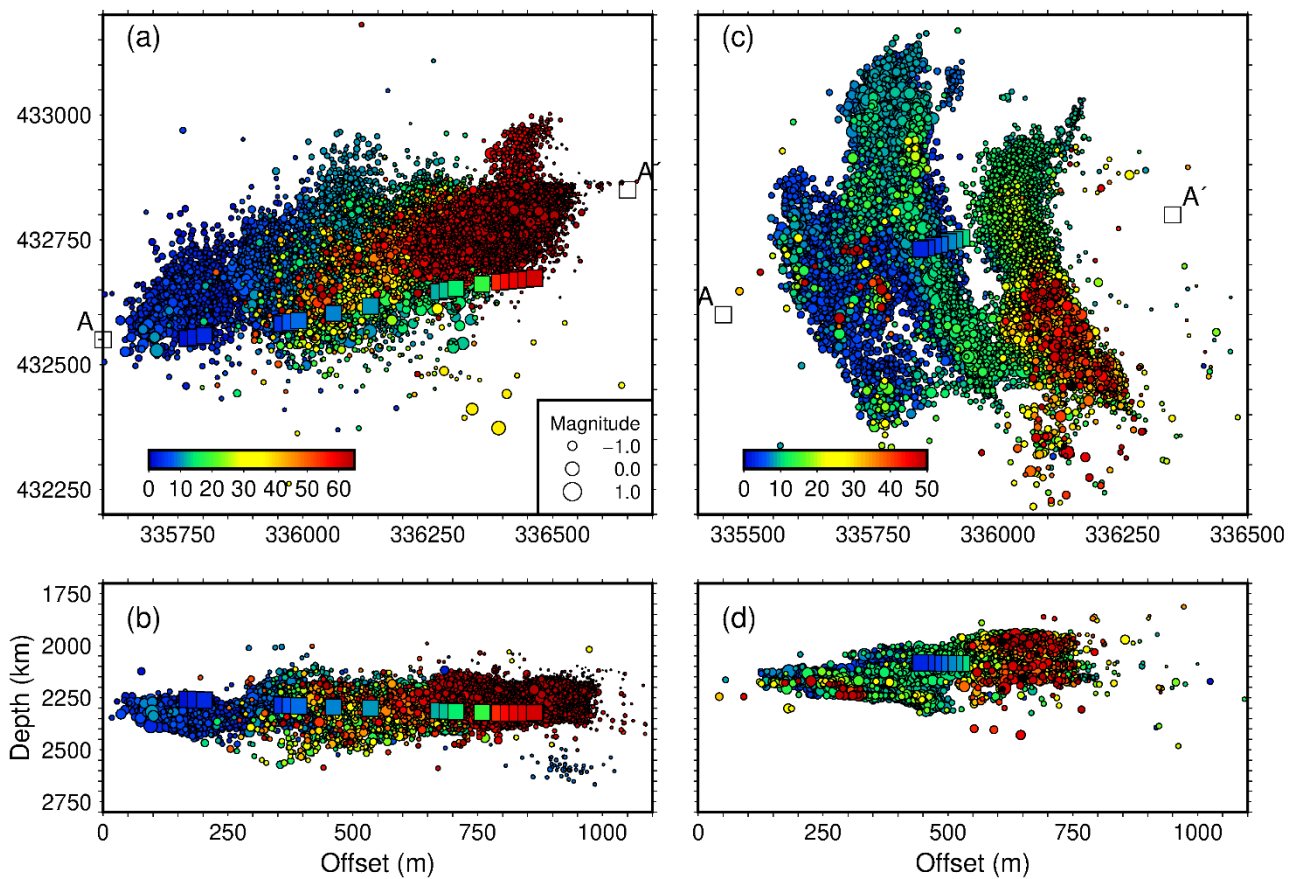




Recent scientific advances in the understanding of induced seismicity from hydraulic fracturing of shales

Multi-Hazards and Risk Programme

Open Report OR/22/050



BRITISH GEOLOGICAL SURVEY

MULTI-HAZARDS AND RISK PROGRAMME

OPEN REPORT OR/22/050

The National Grid and other
Ordnance Survey data
© Crown Copyright and
database rights 2022.
Ordnance Survey Licence
No. 100021290 EUL.

Keywords

Earthquakes, pore pressure,
stress, faults, hazard, risk.

Front cover

Maps of all events in the
microseismic catalogue
recorded during operations in
PNR-1z (a) and PNR-2 (c).
Events are coloured by time in
days from the start of
operations and scaled by
magnitude. Axes show British
National Grid Eastings and
Northings. (b) and (d) show
depth cross-section showing
event depths along the profile
A-A'.

Bibliographical reference

BAPTIE, B., SEGOU, M.,
HOUGH, E. & HENNISSSEN, J. A.
I., 2022.

Recent scientific advances in
the understanding of induced
seismicity from hydraulic
fracturing of shales. *British
Geological Survey Open
Report*, OR/22/050. 51pp.

Copyright in materials derived
from the British Geological
Survey's work is owned by
UK Research and Innovation
(UKRI) and/or the authority
that commissioned the work.
You may not copy or adapt
this publication without first
obtaining permission. Contact
the BGS Intellectual Property
Rights Section, British
Geological Survey, Keyworth,
e-mail ipr@bgs.ac.uk. You
may quote extracts of a
reasonable length without
prior permission, provided a
full acknowledgement is given
of the source of the extract.

Maps and diagrams in this
book use topography based
on Ordnance Survey
mapping.

Recent scientific advances in the understanding of induced seismicity from hydraulic fracturing of shales

B Baptie, M Segou, E Hough and J A I Hennissen

BRITISH GEOLOGICAL SURVEY

The full range of our publications is available from BGS shops at Nottingham, Edinburgh, London and Cardiff (Welsh publications only) see contact details below or shop online at www.geologyshop.com

The London Information Office also maintains a reference collection of BGS publications, including maps, for consultation.

We publish an annual catalogue of our maps and other publications; this catalogue is available online or from any of the BGS shops.

The British Geological Survey carries out the geological survey of Great Britain and Northern Ireland (the latter as an agency service for the government of Northern Ireland), and of the surrounding continental shelf, as well as basic research projects. It also undertakes programmes of technical aid in geology in developing countries.

The British Geological Survey is a component body of UK Research and Innovation.

British Geological Survey offices

**Nicker Hill, Keyworth,
Nottingham NG12 5GG**

Tel 0115 936 3100

BGS Central Enquiries Desk

Tel 0115 936 3143

email enquiries@bgs.ac.uk

BGS Sales

Tel 0115 936 3241

email sales@bgs.ac.uk

**The Lyell Centre, Research Avenue South,
Edinburgh EH14 4AP**

Tel 0131 667 1000

email scotsales@bgs.ac.uk

**Natural History Museum, Cromwell Road,
London SW7 5BD**

Tel 020 7589 4090

Tel 020 7942 5344/45

email bgs_london@bgs.ac.uk

**Cardiff University, Main Building, Park Place,
Cardiff CF10 3AT**

Tel 029 2167 4280

**Maclean Building, Crowmarsh Gifford,
Wallingford OX10 8BB**

Tel 01491 838800

**Geological Survey of Northern Ireland, Department of
Enterprise, Trade & Investment, Dundonald House,
Upper Newtownards Road, Ballymiscaw,
Belfast, BT4 3SB**

Tel 01232 666595

www.bgs.ac.uk/gsni/

**Natural Environment Research Council, Polaris House,
North Star Avenue, Swindon SN2 1EU**

Tel 01793 411500

Fax 01793 411501

www.nerc.ac.uk

**UK Research and Innovation, Polaris House,
Swindon SN2 1FL**

Tel 01793 444000

www.ukri.org

Website www.bgs.ac.uk

Shop online at www.geologyshop.com

Foreword

The Department for Business, Energy & Industrial Strategy (BEIS), the Government department responsible for energy policy, has asked The British Geological Survey (BGS) to produce a short report on “the geological science of shale gas fracturing and the modelling of seismic activity in shale rocks in the UK”. The terms of reference for this review can be found at <https://www.gov.uk/government/publications/review-of-the-geological-science-of-shale-gas-fracturing>. The report is based on peer-reviewed literature and relevant outputs from regulators, focussing on scientific advances since 2019. The report is desk-based and does not include the drilling of new test wells or seismic monitoring.

Acknowledgements

We thank colleagues in the research community, Environment Agency and the North Sea Transition Authority for helpful discussions that informed the report. We also thank Professor W. Ellsworth (University of Stanford, USA), Dr. J. Rubinstein (United States Geological Survey), Dr. Ian Williams (Natural Environment Research Council), J. Ford (British Geological Survey) and Dr. R. Lockett (British Geological Survey) for constructive and helpful reviews. Data for Figure 3 was kindly provided by Tom Kettleby (University of Oxford). Locations for well with stress magnitude measurements in Figure 5 was provided by Mark Fellgett (British Geological Survey).

Contents

- Foreword i
- Acknowledgements i
- Contents ii
- Executive Summary iv
- 1 Introduction..... 1
- 2 Background 2
- 3 Assessing earthquake hazard and mitigating risk 4
 - 3.1 Recent Scientific Advances in Earthquake Monitoring and Forecasting..... 5
 - 3.2 Advances in risk analysis and mitigation 8
- 4 Comparison of HFIS with induced seismicity from other industries 12
 - 4.1 Hydraulic fracturing of shales 12
 - 4.2 Wastewater disposal 13
 - 4.3 Mining 13
 - 4.4 Conventional Oil and Gas Production 14
 - 4.5 Geothermal Energy 14
- 5 Modelling of shales in relation to seismic activity 16
 - 5.1 Recent advances in the modelling of shale successions in the UK 16
 - 5.2 Geomechanics of HF operations: stress state in the UK and fault reactivation potential
18
 - 5.3 Should we expect HFIS in other shales outside of Lancashire? 20
- 6 Global experience of HFIS 22
- 7 Conclusions 26
- Data and Resources..... 28
- Glossary and acronyms 29
- References 31
- Appendix 1: Unconventional hydrocarbon resource and exploration in the UK 41

FIGURES

Figure 1. Seismicity at the epicentral area for 1 year following the 2016 M=6.0 Amatrice earthquake (star) in Italy from the human analyst catalogue using real-time data of the institute responsible for seismicity monitoring (INGV-Italy in this case) (left) and deep learning methods (right). From Beroza, Segou and Mousavi (2021). 6

Figure 2. Seismicity response to hydraulic fracturing at the Preston New Road site. (a-b) Histograms of the number of $M \geq -1.5$ events per hour (black bars) as a function of time during operations along with the cumulative volume of injected fluid (light blue line) at PNR-1z and PNR-2, respectively. For illustration purposes, we inserted a time gap during the pause of operations at PNR-1z, which is indicated by the grey area. (c-e) Examples of seismic productivity and earthquake magnitudes vs. time (red circles) in response to the injection history (light blue line) at selected sleeves. From Mancini et al. (2021). 7

Figure 3. Top: maximum magnitude forecasts for PNR-2 using the seismic efficiency and seismogenic index methods (solid black line and dotted line, respectively). Circles show the events, coloured by magnitude. Bottom: evolution of the b--value (solid blue line), seismic efficiency (solid purple), and seismogenic index (dotted purple). Modified from Kettlety et al., (2020) using data from Kettlety & Butcher (2022) and data provided by Kettlety (pers. comm.). 10

Figure 4. Carboniferous palaeogeography showing the fragmentation of the landmass at the time of deposition of the Bowland Shale Formation. BH = Bowland High; BT = Bowland Trough/Basin, CLH = Central Lancashire High; DH = Derbyshire High; EG = Edale Gulf; GT = Gainsborough Trough; LDH =Lake District High; MH = Manx High; WG = Widmerpool Gulf. (based on Waters et al., 2009; Fraser and Gawthorpe, 2003). Contains Ordnance Survey Data © Crown Copyright and database rights 2022. Ordnance Survey Licence No. 100021290 EUL..... 17

Figure 5. The orientation of the maximum horizontal compressive stress (green vectors) and locations of wells where the magnitude of at least one of the principal stresses has been measured (orange squares). Stress orientations are from the World Stress Map data release 2016 (Heidbach et al., 2018). Locations of sites where stress magnitudes have been measured are from Fellgett et al., (2018). Areas underlain by potentially prospective shale rocks are shaded grey. 20

Figure 6. Global distribution of notable earthquakes induced by hydraulic fracturing (HF). This includes documented cases from the USA (Oklahoma, Texas, Ohio), Canada (Alberta, BC), the UK and China. Locations and magnitudes are from the HiQuake database (Wilson et al., 2017). 23

TABLES

Table 1. Summary of documented cases of hydraulic fracturing induced seismicity reviewed by Schultz *et al.* 2020a. CRET Cretaceous, TRIAS Triassic, PERM Permian, CARB Carboniferous, DEV Devonian; SIL Silurian; ORD Ordovician. HF Hydraulic fracturing; WWI wastewater injection. O: orange; R: red. 25

Executive Summary

The Secretary of State for Business, Energy & Industrial Strategy has commissioned the British Geological Survey to write a short report about seismic activity associated with hydraulic fracturing (HF) of shales to extract hydrocarbons. The specific terms of reference are available at

https://assets.publishing.service.gov.uk/government/uploads/system/uploads/attachment_data/file/1066525/BGS_Letter.pdf. These ask six questions related to recent scientific research on the hazard and risk from induced seismicity during hydraulic fracturing of shale rocks. Our report considers the scientific advances in this area since 2019 that have been published in peer reviewed scientific journals as well as other recent studies commissioned by regulatory authorities. The main conclusions of our report in relation to each of the questions in the terms of reference are as follows:

Forecasting the occurrence of large earthquakes and their expected magnitude remains a scientific challenge for the geoscience community. This is the case for both tectonic and induced earthquakes. (Questions 1 and 2)

Methods to estimate the maximum magnitudes of induced earthquakes based on operational parameters and observed seismicity have been tested using data from both Hydraulic Fracturing (HF) operations and data from other industries. These methods have shown some applicability to guide operational decisions using real-time data. However, they do not currently account for the possibility of events that occur after operations have stopped or earthquakes on faults that extend outside the stimulated volume whose magnitude is not controlled by operational parameters alone. (Questions 1 and 2)

Probabilistic methods widely applied to model and forecast tectonic earthquake sequences show some promise when modified to incorporate information about HF operations and appear capable of providing informative forecasts of the observed earthquake patterns. Operators could make forecasts for operations in new wells using either generic parameters or ones calibrated for operations in adjacent wells. Further testing of these methods may allow them to be further developed for operational scenarios. (Questions 1 and 2)

Enhanced seismicity monitoring and measurement based on machine learning (ML) has been shown to reveal previously undetected earthquakes and hidden faults, essential for both more reliable earthquake forecasts and characterisation of fault reactivation potential. This can compensate for both limited numbers of seismic stations and faults that remain unmapped even by 3D exploration seismic data. (Questions 1 and 2)

Widely used probabilistic methods to assess hazards and risks for tectonic earthquakes can also be applied to induced seismicity. However, there are important differences between how tectonic and induced seismicity evolves in space and time. Recent studies have suggested possible solutions, but further work is needed to develop these models and incorporate them in risk assessments. (Questions 1 and 2)

Traffic light systems remain a useful tool for the mitigation of risks from induced seismicity. New research shows how red-light thresholds can be chosen to reduce the probability of the scenario to be avoided to a required level. This research recommends that there should be sufficient space between the amber and red-light thresholds to ensure that operators have an opportunity to modify operations to mitigate risks. (Questions 1 and 2)

Induced seismicity has been observed in other industries related to underground energy production both in the UK and elsewhere. In the absence of a seismic building code in the UK, consistent risk targets, i.e., scenarios to be avoided, could be considered for all energy related industries that present a risk of induced earthquakes. (Question 3)

Recent research using high quality exploration data that is available for some parts of the UK reveals localised structural and stress heterogeneity that could influence fault reactivation. However, it is not possible to identify all faults that could host earthquakes with magnitudes of up to 3 prior to operations, even with the best available data. (Questions 4 and 5)

Recent research from the USA demonstrates the importance of geomechanical modelling to identify faults that are most likely to rupture during operations. This information can be used to assess risks prior to and during operations. However, these models require accurate mapping of sub-surface faults, robust estimates of stress state, and knowledge of formation pore pressures and the mechanical properties of sub-surface rocks. While this information is available in areas with unconventional hydrocarbon potential such as the Bowland Basin, more data is needed from other basins to apply this more widely (Questions 4 and 5).

Limited exploration data from other basins with unconventional hydrocarbon potential of the UK means that there are significant gaps in our knowledge of sub-surface structure of potential shale resources in these places. (Questions 4 and 5)

The rates of HF-induced seismicity in other countries where shale gas production has been ongoing for many years are observed to vary widely. The limited number of HF operations in the UK means that it is difficult to make a valid comparison of the rates of occurrence of induced seismicity with elsewhere. This underlines the importance of knowledge exchange in monitoring and operational practices. (Question 6)

Our review focusses on recently published geoscience related to induced seismicity caused by HF of shales. Ongoing and future research may bring new insights that may reduce uncertainties and improve mitigation of risks. We did not consider socio-economic research on perception of risks or the benefits of shale gas. Similarly, we do not consider technological advances in hydraulic fracturing.

1 Introduction

The Department for Business, Energy & Industrial Strategy (BEIS), the Government department responsible for energy policy, has asked the British Geological Survey to produce a short report on the “geological science of shale gas fracturing and the modelling of seismic activity in shale rocks in the UK”. The terms of reference for this review can be found at https://assets.publishing.service.gov.uk/government/uploads/system/uploads/attachment_data/file/1066525/BGS_Letter.pdf. These ask the following six questions.

1. Have there been new developments in the science of fracturing? In particular, are there new techniques in use which could reduce the risk and magnitude of seismic events?
2. If there are new techniques, would they be suitable for use in fracturing in the UK, with its specific geology and high population density?
3. Given the new developments in these technologies, how does the seismicity caused by fracturing compare to other forms of underground energy production, such as geothermal and coal mining, or surface activities such as construction? Can you review the evidence on the different "safe" thresholds for activity, whether they remain the correct ones, and whether differences between them remain justified?
4. Has the modelling of geologies such as shale improved in the period since the pause was implemented in 2019? If so, do these improvements mean we could be confident about the modelling of seismic events and their predictability?
5. It is clear, from experience, that the shales drilled into in Lancashire have problematic geology. Are there other sites, outside of Lancashire, which might be at a substantially lower risk of seismic activity, and what level of confidence would we have in our assessment of seismic activity in these areas?
6. Noting our specific geology and population density, how does seismicity from fracturing in the UK compare to other countries e.g., the US?

This report summarises scientific advances since the pause on shale gas extraction in England was implemented in 2019 that is relevant to addressing these six questions. We include peer-reviewed research published in scientific journals, together with relevant technical reports from regulators and public bodies. We also include older research where it is needed to put more recent work in context. We recognise that factors such as the perception of risk in the community are likely to influence the societal acceptance of shale gas, but this topic is outside the scope of the review. Similarly, there may have been other advances in fields outside the expertise of the authors, such as new hydraulic fracturing technologies. These are also outside the scope of this report.

Section 2 provides some background on induced seismicity related to hydraulic fracturing and exploration for shale gas in the UK. Section 3 considers recent research on the assessment of hazard and risk of hydraulic fracture induced seismicity (HFIS) to address questions 1 and 2. We also discuss how risks might be mitigated. Section 4 discusses induced seismicity from mining, conventional oil and gas production, geothermal energy projects and waste-water disposal, and compares this to that associated with HF, to answer question 3. Section 5 considers recent research on the geology of shale rocks in the UK and their susceptibility to induced seismicity to answer question 4. Section 5 also compares the geology of shales in Lancashire with other basins with shale gas potential in the UK to answer question 5. Finally, in section 6, we compare induced seismicity from hydraulic fracturing of shales in the UK, with that observed in the USA, Canada and China, to answer question 6.

Throughout the report, we draw on case studies of published examples of HFIS, including case studies from HF operations in the PNR-1z and PNR-2 wells, Blackpool, Lancashire, analytical and numerical modelling studies, geological investigations, hazard and risk assessments, as well as our wider understanding of earthquakes in general. We also discuss the scientific uncertainties and data gaps that limit our current state of knowledge. A glossary and list of acronyms used in the report is provided to assist clarity throughout the report.

2 Background

Over the last decade, the number of observations of induced earthquakes caused by hydraulic fracturing (HF) operations around the world has increased as the shale gas industry has developed. Data from the USA and Canada suggest that on average, around 1% of HF wells can be linked to earthquakes with magnitudes of 3 or greater, which are generally large enough to be felt by people. However, in some areas of the USA and Canada the percentage of wells associated with induced earthquakes is much higher (>30%). This variability is often explained in terms of geological factors such as proximity to existing faults (Skoumal et al., 2018b; Anderson & Underhill, 2020; Corlett et al., 2018) or formation pore pressure (Eaton and Schultz, 2018; Sibson, 2020).

A recent review of HFIS by Schultz et al., (2020a) summarised the state of knowledge of induced seismicity associated with hydraulic fracturing for shale gas and presents some well-documented case studies, as well as identifying areas for further research. Another recent review by Atkinson et al., (2020) concluded that hydraulic fracturing can trigger earthquakes large enough to cause potentially damaging ground motions and that the hazard from earthquakes induced by hydraulic fracturing might greatly exceed the natural earthquake hazard in regions of low to moderate seismicity.

Exploration for shale gas started in the UK when the first onshore licenses were awarded in 2008 (see Appendix 1). Several shale formations have been identified as having potential for shale gas/oil, and exploration activity has focused on the Bowland Shale Formation and some older Carboniferous-aged shale beds in parts of northern England. In 2011, HF of the first dedicated shale gas well in the UK, Preese Hall 1 (PH-1) near Blackpool, Lancashire, led to felt seismicity (Clarke et al., 2014), the suspension of HF operations, and studies into induced seismicity and risks (Royal Society and Royal Academy of Engineering, 2012). Following this, the UK government published a regulatory roadmap (Department for Business, Energy & Industrial Strategy, 2013) that outlines regulations for onshore shale gas exploration in the UK. These regulations contained specific measures for the mitigation of induced seismicity including avoiding faults during HF; assessing baseline levels of earthquake activity; monitoring seismic activity during and after fracturing; and, using a 'traffic light' system that controls whether injection can proceed or not, based on that seismic activity.

In July 2018, UK Research and Innovation (UKRI), through the Natural Environment Research Council (NERC) and the Economic and Social Research Council (ESRC), funded the Unconventional Hydrocarbons in the UK Energy System programme (UKUH: <http://www.ukuh.org/>). The programme consists of 5 challenge areas of research: (1) the evolving shale gas landscape; (2) shale resource potential, distribution, composition, mechanical and flow properties; (3) coupled processes from reservoir to surface; (4) contaminant pathways and receptor impacts; and (5) socio-economic impacts. The latter consisted of three separate projects: (1) the dynamics of public attitudes and community responses to shale gas; (2) the social construction of unconventional gas extraction; and (3) 'Fracking', framing and effective participation. The programme is scheduled to conclude in Autumn 2022 and to date has resulted in a body of new research that details some geological aspects, including induced seismicity, that are relevant to this review.

In late 2018, HF of the Bowland Shale Formation was carried out in the Preston New Road (PNR)-1z well near Blackpool. Operations were accompanied by seismicity and the largest event, with a magnitude of 1.6 ML, was felt by a small number of people near the epicentre. HF operations in the adjacent PNR-2 well started on 15 August 2019 and were also accompanied by seismicity. The largest of these events had a magnitude of 2.9 ML and occurred on 26 August 2019 at 07:30 UTC, almost 72 hours after the last HF stage on 23 August (Clark et al., 2019). The earthquake was strongly felt at distances of up to a few kilometres from the epicentre (Edwards et al., 2021) and led to a premature end to operations in the PNR-2 well with only 7 of the planned 47 HF stages completed. Following a review of these events (Oil and Gas Authority, 2019), a moratorium on shale gas hydraulic fracturing was implemented on 2 November 2019.

In March 2020, the Oil & Gas Authority (OGA), now the North Sea Transition Authority (NSTA), commissioned four studies to investigate seismicity resulting from hydraulic fracturing operations in PNR-2. The OGA concluded that “it is not yet possible to accurately predict the seismic response to hydraulic fracturing, if any, in relation to variables such as site characteristics, fluid volume, rate or pressure. Where induced seismicity has occurred, mitigation measures have shown only limited success, and there can only be low confidence in their effectiveness currently”, and “there remain significant uncertainties and challenges related to the prediction and management of induced seismicity from hydraulic fracturing”.

3 Assessing earthquake hazard and mitigating risk

In this section, we describe recent scientific advances in earthquake monitoring and forecasting that have had a direct impact on assessing hazard from induced seismicity, along with approaches for estimating risks and mitigating the effects of induced seismicity. We use this to address questions 1 and 2 in the terms of reference. Key findings include

Forecasting the occurrence of large earthquakes and their expected magnitude remains a significant challenge for the geoscience community.

Recent research describes methods that may provide informative forecasts of HFIS in the near future. These forecast models could use parameters from nearby sites in the very early stages of operations, which could then be refined during operations.

The applicability of such methods depends on high-resolution seismicity data such as is available from operations at PNR. The applicability in near-real-time depends on rapid processing of data which is now possible using more advanced artificial intelligence workflows.

Recent research demonstrates that machine-learning can be applied retrospectively, or in near-real-time, to provide the high-resolution data required to support these forecast models.

Probabilistic methods to assess hazards and risks for tectonic earthquakes that combine models of seismicity with models of ground motion, exposure, and vulnerability, can also be applied to induced seismicity.

Red-light thresholds for traffic light systems can be chosen to reduce the probability of the scenario to be avoided to a required level.

Quantitative assessment of the hazard and risk from tectonic earthquakes has been an important area of research for several decades (see Baker, Bradley & Stafford, 2021 for a comprehensive treatment of this subject). In countries where the hazard is high, this has allowed mitigation of risk, primarily through the earthquake resistant design of buildings and other structures, and national building codes enforced by law. Due to its very low seismic hazard, the UK has no (counter-) seismic building code enforced as law for residential buildings. Furthermore, in countries such as the USA, where induced seismicity has increased recently, national seismic hazard maps have been created that include one-year forecasts of induced seismicity (e.g., Petersen et al., 2016).

Following the magnitude 5.5 Mw earthquake in 2017 induced by operations at the geothermal site near Pohang, South Korea (see Section 4.5), Lee et al., (2019) concluded that a comprehensive risk-based approach is required to address the potential for triggering large earthquakes. Similar conclusions have been reached in recent research on induced seismicity from HF operations (Schultz et al., 2021).

The spatial and temporal distribution of induced seismicity is of fundamental importance for the estimation of hazard and risk. Previous studies have shown that most HF-induced earthquakes tend to be within few kilometres of the wellbore where HF has taken place (e.g., Skoumal et al., 2020). In many cases, seismicity is observed to occur within a few hundreds of meters of lateral sections of the well (e.g., Eyre et al., 2019), as is the case with the events observed in Lancashire (Clarke et al., 2014, 2019). These distances seem consistent with the expected sizes of fracture systems stimulated by operations that might connect with existing faults (Shen et al., 2019). However, sometimes, the separation between a well and the observed seismicity is greater, or in some cases it is difficult to establish the connection between a particular well and the diffuse seismicity due to monitoring constraints. Schultz et al., (2015) and Skoumal et al., (2015a) find induced seismicity that is 1 km below the target formation, within the crystalline basement. Similarly, (Bao & Eaton (2016) and Schultz & Wang (2020) find that induced seismicity is laterally offset from the nearest HF stage by over 1 km, well beyond the plausible extent of HF growth (Davies et al., 2013).

HF induced seismicity typically shows a rapid response to HF stimulation with earthquake rates peaking during periods of injection. Schultz et al. (2018) suggest that up to 90% of induced events occur during stimulation, and in many cases, seismicity clearly correlates with individual HF stages (Clarke et al., 2019; Eaton et al., 2018; Yu et al., 2019). However, in some cases, delays of several hours or more have been observed between stage stimulation and the largest earthquakes. This is often referred to as “trailing” or “runaway” seismicity and creates a particular problem as the largest magnitude events can occur after HF operations stop (Clarke et al., 2019; Meng et al., 2019; Schultz et al., 2017).

Induced earthquakes, including those created during HF stimulation, follow the Gutenberg Richter law (Text Box 1) which is universally observed for tectonic earthquakes (Van der Elst et al., 2016; Mancini et al., 2021). This suggests that the magnitudes of the induced events follow a similar scaling relationship to those for natural events. For tectonic earthquakes, which are often considered to be stationary, i.e., their probability distribution function doesn't change with time, this gives us a means to estimate the likelihood of larger earthquakes from a sample of events. However, we need to be very careful about making predictions about the occurrence of events with larger magnitudes. Schultz et al. (2022) show that induced seismicity also follows another empirical relationship observed for induced seismicity (Bath's Law) and use this to build a conceptual framework for statistical bounds on how induced earthquake sequences stop.

From the above, it is clear that our ability to evaluate and mitigate risks from HFIS is directly related with our capability to observe and monitor inherently small magnitude events and predict their occurrence in a relatively short time window during HF operations.

3.1 RECENT SCIENTIFIC ADVANCES IN EARTHQUAKE MONITORING AND FORECASTING

Understanding under what conditions large earthquakes occur and providing advance notice of populations at risk from natural (tectonic) and man-made (induced) earthquakes, is linked with how robustly scientists can identify patterns that emerge from observational data. The predictive task of estimating the probability of occurrence of events above a predefined magnitude threshold and time window, is known as earthquake forecasting. The ability to make robust forecasts depends on the quality of available data, specifically, the availability of high-resolution earthquake catalogues that contain the times of occurrence, locations, magnitudes, and other attributes of even the smallest, unfelt earthquakes.

Deep learning is a type of computational method that uses complex hierarchical models to mimic how humans learn new information. In seismology, recent work has shown that deep learning methods can detect and locate many more earthquakes than conventional algorithms or human analysts (Beroza et al., 2021). Results from recent testing in Italy (Figure 1), Oklahoma, and California (USA) show that at least ten times more earthquakes are detected when using the same input data (Tan et al., 2021). These dramatically more comprehensive and accurate earthquake catalogues can be used to help improve our understanding earthquake behaviour. As a result, this approach has potential for monitoring hydraulic fracturing operations and improving seismicity forecasts.

A recent study by Park et al., (2020) shows how the implementation of deep learning algorithms in central Arkansas illuminated the structure of the Guy-Greenbrier (GB) earthquake sequence, which involved activity on different faults near wastewater disposal wells. Park et al. (2020) show how deep learning detection algorithms can be used to connect seismicity and specific wells by detecting previously hidden events and illuminating paths between faults. In particular, the new machine learning-based detections revealed that the GB sequence consisted of two sequences and that the second sequence may have been triggered by a wastewater disposal well that hadn't previously been considered. Another recent case study of the Delaware basin (Texas, USA) by Sheng et al. (2022) employs the deep learning algorithm, Earthquake Transformer (Mousavi et al., 2020), to detect shallow induced seismicity and show that it is related to the injection of wastewater in nearby wells.

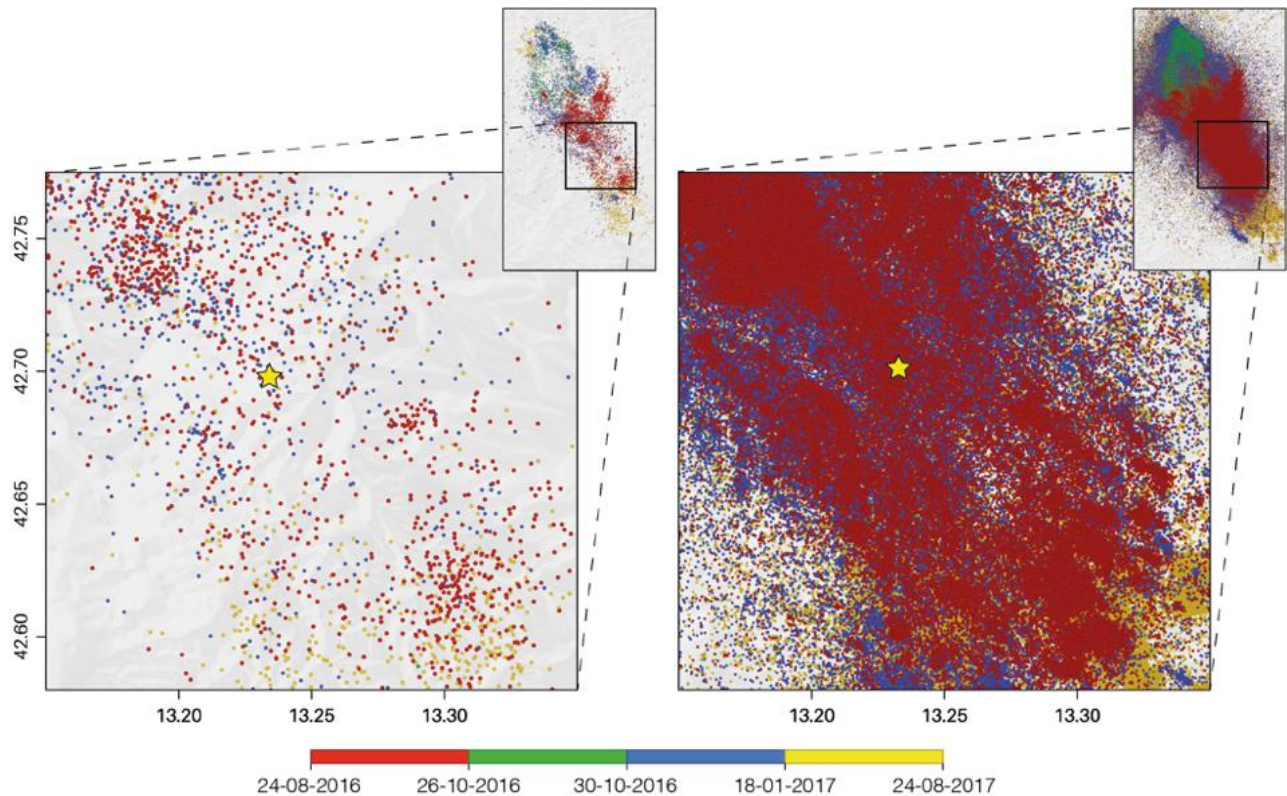


Figure 1. Seismicity at the epicentral area for 1 year following the 2016 M=6.0 Amatrice earthquake (star) in Italy from the human analyst catalogue using real-time data of the institute responsible for seismicity monitoring (INGV-Italy in this case) (left) and deep learning methods (right). From Beroza, Segou and Mousavi (2021).

An additional benefit from analysing previous recordings is the ability to unveil previously hidden seismicity and to trace unknown faults in the vicinity of sites of interest. For example, the application of deep learning algorithms to seismic data from Oklahoma and Kansas (USA) by Park et al., (2022) detected over twenty times more events than previously. The resulting patterns of seismicity revealed activated faults and other large-scale geological features and may contribute to improved estimations of seismic hazard in the region. Geodetic data, such as INSAR satellite imagery, have also been employed to constrain further slip patterns of moderate-sized ($M > 4.0$) HF-induced earthquakes. Wang et al., (2022) used Sentinel-1 satellite imagery to analyse three shallow earthquakes between 2017 and 2019 in the Changning field (China) and found that they were located above the shale formation rather than being associated with deep basement-rooted faults. This is an important finding since the shallow depth of those earthquakes leads to increased expected ground motions.

Earthquake forecast models as developed for natural seismicity estimate the number of expected earthquakes within a given space and time window (e.g., Jordan et al., 2011). In their standard form, they are based on well-established empirical statistics of earthquake occurrence that they are applied to earthquake sequences from around the world. In the field of induced seismicity, early work by Llenos and Michael (2013), used statistical forecast models to explain the observed increase in seismicity in Oklahoma and Arkansas (USA) This was mostly related with wastewater disposal operations, and demonstrated that the change in earthquake rate after injection started is statistically significant, and both the background rate of independent earthquakes (before their time period of interest) and the aftershock productivity must increase after operations. Both regions in USA had low but steady earthquake rates of approximately 2 events per year (above $M > 2.5$), comparable to the observed seismicity rates in the UK.

Physics-based forecast models developed for induced seismicity caused by wastewater-disposal in the USA have continued to improve (e.g., Rubinstein, 2021). These physical models often assume that seismicity is driven by the rate of injection-induced pressure increases at any given location and spatial variations in the number and stress state of basement faults affected by the pressure increase (Langenbruch et al., 2018). Such physics-based forecast models can be used to estimate hazards from future injection scenarios and could be customized for HF-induced seismicity.

Mancini et al. (2021) also use a statistical model originally developed for tectonic sequences to model the induced seismicity during HF operations at Preston New Road. This took advantage of the rich catalogue of events recorded by downhole geophone arrays at the Preston New Road site. Mancini et al. (2021) tested the ability of standard models and modified models that accounted for fluid injection rates to track the evolution of seismicity during operations. They also used the model for PNR-1Z to make an out-of-sample forecast for the PNR-2 seismicity. Figure 2 shows the seismicity rate response during operations as a function of operational parameters, such as the injection volume. Mancini et al., (2021) concluded that “operators could provide forecasts during the very early stages of operations using parameters that are either generic or calibrated on adjacent wells”, and that “injection-rate driven statistical forecast models produce informative time-dependent probabilistic seismic rate forecasts.”

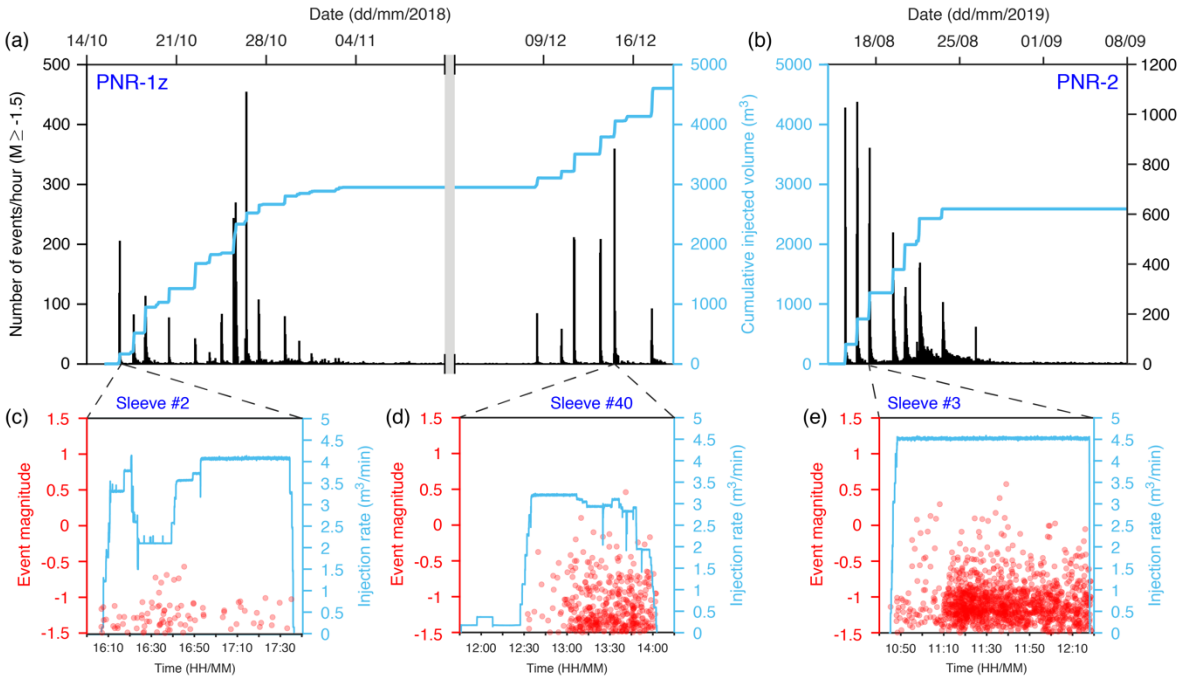


Figure 2. Seismicity response to hydraulic fracturing at the Preston New Road site. (a-b) Histograms of the number of $M \geq -1.5$ events per hour (black bars) as a function of time during operations along with the cumulative volume of injected fluid (light blue line) at PNR-1z and PNR-2, respectively. For illustration purposes, we inserted a time gap during the pause of operations at PNR-1z, which is indicated by the grey area. (c-e) Examples of seismic productivity and earthquake magnitudes vs. time (red circles) in response to the injection history (light blue line) at selected sleeves. From Mancini et al. (2021).

Text Box 1: Earthquake magnitudes and the Gutenberg Richter Law

The relationship between the magnitude and number of tectonic earthquakes are universally observed to follow an empirical relationship between an earthquake's magnitude and its frequency of occurrence known as the Gutenberg-Richter (GR) law (Gutenberg and Richter, 1954). The GR law can be expressed as:

$$\log_{10} N = a - bM \quad (1)$$

where, N is the number of earthquakes with a magnitude of $\geq M$. The constant a is a function of the total number of earthquakes in the sample and is known as the earthquake rate. The constant b gives the proportion of large events to small ones and is commonly referred to as the b -value. In general, b -values are close to unity for tectonic earthquakes, so for each unit increase in magnitude, the number of earthquakes reduces tenfold. Induced earthquakes also follow the GR law suggesting that the magnitudes of the induced events are controlled by similar processes to those of natural events (Van der Elst et al, 2016; Mancini et al., 2021).

Although the GR law gives us a means to estimate the likelihood of larger earthquakes from a sample of events, we need to be very careful about making predictions about the occurrence of events with larger magnitudes. This is because the GR distribution is a power law and heavy tailed, leading to possible outliers with very high values. If magnitudes are drawn randomly from the GR distribution, the probability of sampling a magnitude more than a given value increases with sample size. This is known as the sample size hypothesis (van der Elst et al., 2016). The distribution for M_{\max} is also heavy tailed.

Induced seismicity obeys Båth's law, an empirical observation that the average magnitude difference between a mainshock earthquake and its largest aftershock is approximately 1.2 magnitude units.

3.2 ADVANCES IN RISK ANALYSIS AND MITIGATION

Edwards *et al.*, (2021) presented a retrospective seismic risk analysis applied to the largest of the induced events observed at Preston New Road. Open source freely available software (Silva *et al.*, 2014) was used to calculate the damage distribution for spatially variable ground-motions for different earthquake magnitudes calculated using empirical Ground Motion Prediction Equations (GMPEs) developed for induced seismicity (Atkinson, 2015). GMPEs (e.g., Douglas and Edwards, 2016) predict values of a particular ground-motion parameter, such as peak ground acceleration (PGA) or peak ground velocity (PGV), as a function of independent variables such as the magnitude and depth of the earthquake, the distance to the site and the ground conditions at the site of interest. Edwards *et al.*, (2021) incorporate both the exposure and fragility of different building types to different levels of ground shaking. The mean modelled occurrences of cosmetic and minor structural damage are consistent with reported damage. Edwards *et al.*, (2021) conclude that significant occurrences of minor to major structural damage are likely for magnitudes in the range 3.5 to 4.5 ML.

While mitigation of the risk of tectonic earthquakes has largely taken the form of earthquake-resistant design based on long-term probabilistic estimates of seismic hazard, mitigation of risk of induced earthquakes has attempted to reduce the hazard through operational controls such as limiting the rate or volume of injected fluid.

Traffic light systems (TLS) are one of the most widely implemented means of attempting to mitigate the risk of induced earthquakes from HF or other operations that involve subsurface injection (e.g., Baisch *et al.*, 2019). It is worth noting that despite widespread implementation, TLS have often had limited success (Bommer *et al.*, 2015; Baisch *et al.*, 2019). TLS are essentially control systems that allow for low levels of induced seismicity but set a stopping point (red-light) for operations to reduce the probability of events that may result in a concern for public health and safety. Verdon and Bommer (2021) state that the design of a TLS should consider three questions:

1. What is the risk target in terms of consequences to be avoided?
2. Which hazard metric is the best indicator of the risk potential?
3. What threshold of the hazard metric will ensure risk targets are not exceeded?

The risk target could be avoiding ground motions that cause disturbance or nuisance (e.g., Cremen and Werner, 2020) or those that might result in damage to buildings or other infrastructure. The choice of the risk target is a decision related to acceptable risks.

Widely used hazard metrics are the intensity of ground motion or the earthquake magnitude. Since the intensity of the ground motions can be directly related to the impact of the earthquake in terms of perceptibility, it may seem an obvious choice. However, recorded earthquake ground motions show strong spatially variability, so the largest ground motions may not be recorded without a dense network of sensors. This is further complicated if sensors are in environments where background noise levels may exceed the signals of interest. Schemes using earthquake magnitudes may be simpler to implement, although there are also challenges associated with magnitude estimation (Kendall et al., 2019) and accounting for uncertainties (Roy et al., 2021).

Schultz et al. (2020b) use a probabilistic assessment of risk for choosing traffic light thresholds that incorporate probabilistic maximum magnitudes, GMPEs, population densities, site amplification factors, and felt or damaging ground-motion thresholds to compute the risk of damage or nuisance. Schultz et al., (2020b) suggest that TLS red-light thresholds should be set within the nuisance range of ground motions that reduce the chances of unacceptable damage and that setting amber-light thresholds two magnitude units less than the red light gives operators sufficient opportunity to implement mitigation strategies. The authors note that the largest source of uncertainty is the way that trailing seismicity, earthquakes that occur after operations stop, is modelled.

Schultz et al. (2021) use a similar approach to show how TLS red lights can be geographically tuned to account for how shaking may translate to structural damage, arguing that this is fairer and safer than a single threshold applied over a broad area. This essentially means low thresholds in more populated regions.

Verdon and Bommer (2021) use HFIS data from around the world to examine magnitude jumps and trailing events that occur after operations stop. They find that in most cases magnitude jumps, i.e., sharp increases in magnitude from preceding events within a sequence, are less than 2 magnitude units, with the largest being 1.6. Post-injection magnitude increases were observed in 25% of cases but these increases generally occurred soon after injection, with most cases showing no increase in magnitude more than a few days after the end of injection. Verdon and Bommer (2021) go on to suggest that TLS may require red-light thresholds as much as two magnitude units below the threshold that the scheme is intended to avoid.

Several authors have suggested modifications to TLS to improve performance. For example, Mignan et al., (2017) propose a data driven, adaptive traffic light system (ATLS) based on a statistical forecasting system to provide a risk-based safety target model of induced seismicity. Kwiatek et al., (2019) use near-real-time information on induced-earthquake rates, locations, magnitudes, and evolution of seismic and hydraulic energy by reducing well-head pressures or flow rates to control injection-induced seismicity.

The relationship between the rate or volume of injected fluid and induced seismicity has been widely debated over the last decade or more. McGarr (2014) propose that the maximum magnitude of earthquakes induced by fluid injection is limited by the injected volume and that the maximum magnitude increases with injected volume. Schultz et al. (2018) found that injection volume was the key operational parameter correlated with induced earthquakes in the Duvernay Formation in the Alberta Basin, Canada. In the Horn River Basin (British Columbia), larger earthquakes only occurred when the total monthly injected volume across the basin exceeded 150,000 m³ (Farahbod et al., 2015). In other areas, such as the Eagle Ford lay in Texas, the volume of injected fluid per unit area per day was seen to be an important factor in the rate of induced seismicity associated with HF (Fasola et al., 2019). However, other authors (e.g., Atkinson et al., 2016, Ellsworth et al., 2019; Lee et al., 2019; Keranen & Weingarten, 2018) have shown that this limit does not always hold, or that maximum magnitudes are consistent with sampling from an unbounded Gutenberg-Richter distribution (Van der Elst et al., 2016). Atkinson (2020) notes that earthquakes with magnitudes greater than around 2 result

from slip on existing faults that are triggered by stress changes caused by the injection of fluid during the HF process. Since such faults may extend outside the hydraulically fractured zone, the maximum magnitude will be controlled by local geology and tectonics, not operational parameters such as the amount of injected fluid. In this report, we discuss in detail how and under which conditions operational parameters influence the fault behaviour and its slip potential that reflects the ability of the fault to move (slip) causing an earthquake (See Section 5.2)

Shapiro et al., (2010) and Shapiro (2018) suggest that a *seismogenic index* (SI) can be used to compare the rate of induced seismicity in different environments. This relates the number of events above a given magnitude to the injection volume but is independent of other injection parameters and depends only on tectonic features. Hallo et al., (2014) follow a similar approach to McGarr (2014) and relate cumulative seismic moment release to injected volume using a scaling parameter called the *seismic efficiency* (SE). Hallo et al. (2014) combine the SE parameter with the Gutenberg-Richter law to estimate the magnitude of the largest induced earthquake. Verdon and Budge (2018) and Clark et al. (2019) use a statistical model in which the rate of induced seismicity scales with the injection volume to retrospectively forecast expected event magnitudes during HF operations from the Horn River Shale, Canada and Preston New Road (PNR-1z), UK.

Kettlety et al., (2020) use both the seismic efficiency (Hallo et al., 2014) and seismogenic index (Shapiro et al., 2010) methods to retrospectively estimate maximum magnitudes using microseismic data during operations at PNR-2 (Figure 3). They find that overall, the SE method slightly underpredicts the magnitude of the largest observed earthquake (2.9 ML), while the SI method consistently overpredicts the observed magnitudes.

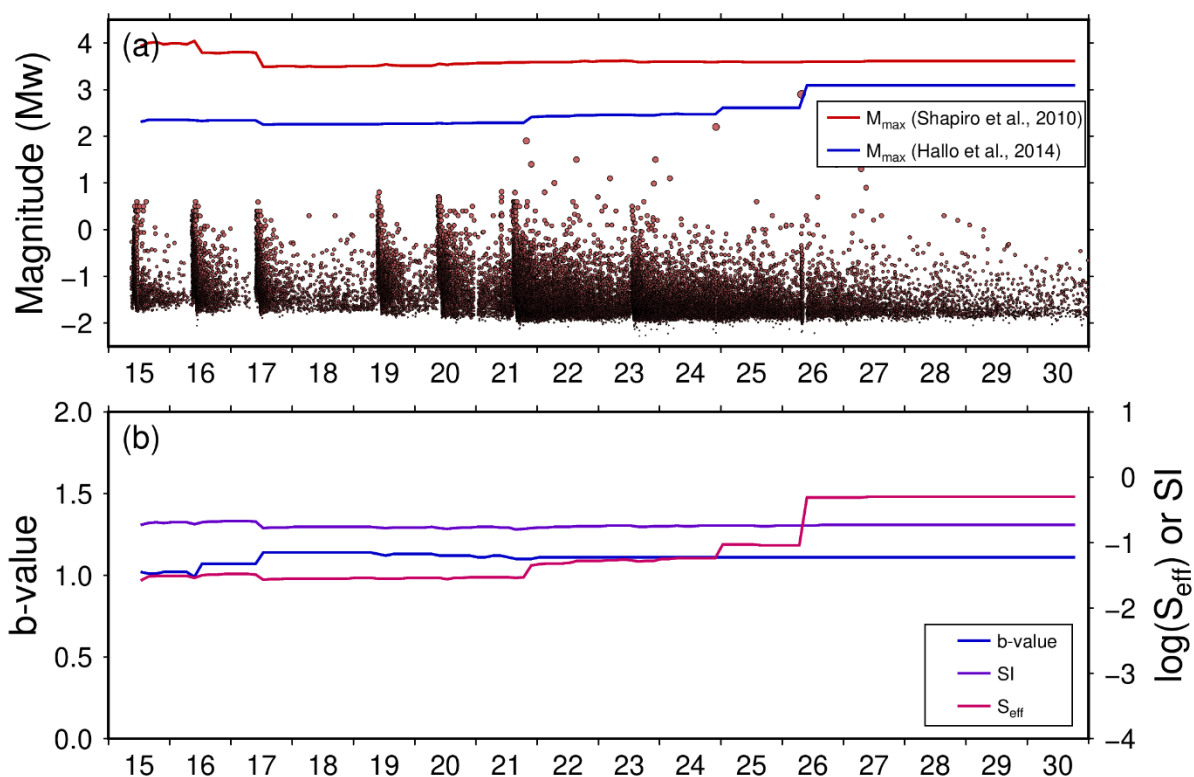


Figure 3. Top: maximum magnitude forecasts for PNR-2 using the seismic efficiency and seismogenic index methods (solid black line and dotted line, respectively). Circles show the events, coloured by magnitude. Bottom: evolution of the b-value (solid blue line), seismic efficiency (solid purple), and seismogenic index (dotted purple). Modified from Kettlety et al., (2020) using data from Kettlety & Butcher (2022) and data provided by Kettlety (pers. comm.).

Cremen and Werner (2020) combine the Hallo *et al.* (2014) injection-volume-based statistical model of event magnitudes with a ground motion prediction equation (Cremen *et al.*, 2019), and an exposure model, to quantitatively link the volume of fluid injected with the potential for nuisance felt ground motions during HF operations at Preston New Road. Their results suggest that ground motions equivalent in amplitude to that at which pile driving becomes perceptible, may be exceeded in the location of at least one building for event magnitudes equal to or exceeding the current UK induced seismicity traffic light system “red-light” event of 0.5 ML, or injection volumes $\geq 1000 \text{ m}^3$. Cosmetic damage may occur in at least one building for $M_w \geq 2.1$ or injection volumes $\geq 40,000 \text{ m}^3$. Cremen and Werner (2020) suggest that this framework facilitates control of the injection volume ahead of time for risk mitigation and can be used to inform policy related to HFIS.

4 Comparison of HFIS with induced seismicity from other industries

In this section, we compare HFIS with induced seismicity from other forms of underground energy production, such as geothermal operations and coal mining to answer question three. We also discuss any regulatory measures that have been used in these industries. Much of this research pre-dates HF operations. Key findings include

Induced seismicity has been observed in other industries that have been used for energy production in UK.

In the absence of a seismic building code in the UK, consistent risk targets, i.e., scenarios to be avoided, could be considered for all energy related industries that present a risk of induced earthquakes.

Adaptive traffic light systems to mitigate the risks of induced seismicity have been successfully used in the geothermal industry. Similar systems could be used during HF operations.

It is relatively well-known that anthropogenic activity can result in man-made or “induced” earthquakes. Although such events are generally small in comparison to natural earthquakes, they are often perceptible at the surface, and some have been quite large. Underground mining, deep artificial water reservoirs, oil and gas extraction, geothermal power generation (enhanced geothermal systems and deep hydrothermal projects) and waste disposal have all resulted in cases of induced seismicity. Several prior review articles and reports have addressed this issue (e.g., Davies *et al.*, 2013; Ellsworth 2013; Grigoli *et al.*, 2017; Keranen and Weingarten, 2018). These activities all have the potential to change the state of stress, which can induce or trigger slip on faults within the Earth. The connection between human activity and induced seismicity is usually based on both a spatial and temporal coincidence, although this is not always clear.

4.1 HYDRAULIC FRACTURING OF SHALES

In 2011, HF of the first dedicated shale gas well in the UK, PH-1, led to felt seismicity (Clarke *et al.*, 2014), the suspension of HF operations, and inquiries into induced seismicity and risks (Royal Society and Royal Academy of Engineering, 2012). The largest seismic event, on 1 April 2011, had a magnitude of 2.3 ML and was felt by people close to the epicentre, and was associated with wellbore deformation. Clarke *et al.*, (2014) concluded that the earthquake activity was caused by fluid injection directly into a nearby fault zone.

The UK government (BEIS, 2013) published a regulatory roadmap that outlines regulations for onshore oil and gas (shale gas) exploration in the UK. These regulations contain specific measures for the mitigation of induced seismicity including: avoiding faults during hydraulic fracturing; assessing baseline levels of earthquake activity; monitoring seismic activity during and after fracturing; and, using a TLS that controls whether injection can proceed or not, based on that seismic activity. Similar regulatory measures to mitigate the risk of HFIS are also in place in the USA and Canada although specific TLS vary by state or province and thresholds are generally higher.

In the UK, the red-light TLS threshold of 0.5 ML for the cessation of operations is considerably less than the limits in California (2.7 ML) and Illinois, Alberta and British Columbia (4.0 ML), making it the most conservative red-light threshold in any jurisdiction where HF operations have been carried out (Schultz *et al.*, 2020b). This threshold was chosen so that the probability of a 2.5 ML event, which would likely be felt by people close to the epicentre, would be approximately 0.01. However, in contrast to TLS used for HF operations elsewhere, the UK regulations allowed operators to continue HF after a brief pause following an event that exceeded the red-light threshold, rather than a complete cessation of operations in that well. This meant that the red-light threshold became an amber one, since it did not impose a permanent suspension of operations.

4.2 WASTEWATER DISPOSAL

Dramatic increases in induced seismicity in central and eastern U.S. and Canada over the last ten years have been linked to both long-term disposal of large volumes of wastewater from oil and gas production in Class II Underground Injection Control (UIC) boreholes (Ellsworth, 2013; Rubinstein and Mahani, 2015; Walsh and Zoback, 2016). Some of the wastewater is from hydraulic fracturing for shale gas production. This has resulted in a considerable body of new research on seismicity related to fluid injection. In addition, several of the largest earthquakes in the US midcontinent in 2011 and 2012 may have been triggered by this process (e.g., Horton, 2012; Kim, 2013), suggesting that wastewater disposal by injection in deep boreholes poses a significant seismic risk. The two largest of these were the magnitude 5.7 Prague earthquake in 2011 (Kerenan et al., 2013) and the magnitude 5.8 Pawnee earthquake (Manga et al., 2016), both in central Oklahoma. The latter destroyed 14 homes and injured two people. As a result of this, regulations were introduced to limit the volume of fluid that could be disposed in this way. Seismic hazard forecasts for the Central and Eastern United States (CEUS) now include contributions from both induced and natural earthquakes (Peterson et al., 2016). In Texas, current regulations also require a pre-drilling risk assessment for new wastewater disposal wells that includes estimating fault reactivation potential using a method developed by Walsh & Zoback (2016).

As a result, Oklahoma regulators called for a 40% reduction in the volume of injected wastewater in 2016 from the volume injected in 2014. Such regulations are already bringing about a reduction in the number of induced earthquakes. Langenbruch and Zoback (2016) present a statistical model of how seismicity is expected to decrease and suggest that seismicity may return to background levels within a few years. However, aftershock sequences associated with larger events are likely to delay the rate of seismicity decrease in those areas.

4.3 MINING

Mining-induced seismicity has been observed in underground mining and tunnelling projects worldwide, where the excavation of large volumes of rocks at depth results in stress changes that can cause fracture initiation and propagation, as well as reactivation of existing faults. Such seismicity has been observed in a wide range of geological and mining environments including the gold mines of South Africa (Cook, 1976), iron ore mines of Sweden (Ma et al., 2018) and southwest Poland (Kozłowska et al., 2021) and the coal mines in the Ruhr, Germany (Bischoff et al., 2010) and Upper Silesia, Poland. Mining-induced seismic events rarely exceed magnitude of 5 or above. However, there are examples of mining-induced earthquakes with magnitudes large enough to have caused ground shaking that resulted in fatalities, structural damage to buildings at the surface and on some occasions, casualties.

The coalfields of Britain have frequently been the source areas of small to moderate earthquakes and tremors in these areas have been reported for over one hundred years (Davison, 1919). Analyses of instrumental recordings (e.g., Redmayne, 1988) led to the conclusion that these events were closely related in space and time to ongoing mining activity. In the 1980's and 1990's mining events accounted for approximately 25% of all the earthquakes recorded in the UK (Browitt et al., 1985). Since the rapid decline of mining activity in the UK there has been a sharp decrease in the number of these events.

The maximum observed magnitudes from coal mining induced seismicity in the UK is around 3 ML (Bishop et al., 1993 and Redmayne et al., 1998). The three largest events each had magnitudes of 3.1 ML and occurred in Mansfield and Stoke-on-Trent. These were felt with an intensity of 4 EMS. However, other mining induced earthquakes with smaller magnitudes have been felt with higher intensities, for example, a magnitude 2.3 ML event at Rosewell in Midlothian was felt with an intensity of 5 EMS.

There was no specific regulation in the UK that required mine operators to mitigate the risks of induced seismicity.

4.4 CONVENTIONAL OIL AND GAS PRODUCTION

There are numerous examples of induced earthquakes in hydrocarbon fields related to oil and gas production (e.g., Suckale; 2009, 2010). These are often a response to long-term production, where the extraction related subsidence results from compaction of the reservoir leading to activation of faults around the reservoir (e.g., Van Eijs et al., 2006). Early observations include a series of earthquakes that were felt near the Goose Creek oil field in south Texas. Oil production there caused the field to subside by as much as 1 m between 1917 and 1925 (Pratt and Johnson, 1926). A sequence of earthquakes was recorded at the Wilmington oil field, California (Kovach, 1974), where subsidence between 1936 and 1966 reached 9 m. Most induced or triggered earthquakes in hydrocarbon fields have small or moderate magnitudes. In the North Sea, a magnitude 4.4 Mw earthquake that occurred in the Ekofisk field in 2001 was conclusively linked to oil production (Ottemöller et al., 2005).

Seismicity observed at the Groningen gas field in the Netherlands is one of the best understood examples of induced seismicity related to conventional hydrocarbon production in Europe (Grigoli et al., 2017). The field is an area where there is little evidence of historical earthquake activity, and the area is considered to be tectonically stable. Seismicity induced by gas extraction operations started in 1986 (around 20 years after the start of production). Seismic activity continued to increase with time and reached a maximum in 2013, causing considerable public concern. The largest event was a magnitude 3.6 Mw earthquake on 16 August 2012. The earthquakes have resulted in considerable damage as a result of the shallow depths of the earthquakes (3 km) along with the near surface geology of clay, peat and sand, as well as the buildings not being designed with earthquake shaking in mind due to the very low natural seismicity rates.

Numerous papers have been written on the seismicity at Groningen and its relation to gas production (e.g., Bourne et al. 2014, 2018; Van Thienen-Visser and Breunese, 2015; Nepveu et al. 2016; Dempsey and Suckale 2017). Overall, there is a consensus that the observed seismicity is a result of stress changes resulting from depletion of the reservoir, which leads to increases in shear stress on faults systems in and around the depleted reservoir (e.g., Bourne, 2014; Van Thienen-Visser and Breunese 2015).

In 2014, the Dutch government introduced legislation to set limits on the produced volume of gas. As a result, production fell sharply in the following years. An annual limit of 24 bcm for the period 2017-2021 was set in 2016. However, despite these reductions, seismicity remained at an elevated level, and following a magnitude 3.4 quake in January 2018, the Dutch government decided to further lower annual extraction within 5 years to at most 12 bcm and to end the operation of the Groningen field altogether by 2030. At the same time, the Dutch government also introduced legislation that allowed properties owners to submit claims for compensation for physical damage caused by the induced earthquakes to be settled by the operator, NAM (Nederlandse Aardolie Maatschappij BV, a joint venture of Shell and ExxonMobil).

There is no specific regulation in the UK that requires operators to mitigate the risks of induced seismicity from conventional oil and gas production.

4.5 GEOTHERMAL ENERGY

There are examples of induced seismicity in both Enhanced Geothermal Systems (EGS) and natural hydrothermal fields. EGS aims to improve productivity by hydraulic fracturing of intact rock (high pressure injection), hydraulic shear stimulation of existing flow paths or fractures (low pressure injection), thermal stimulation, and/or chemical stimulation (e.g., Allis, 1982). By contrast, in natural geothermal fields productivity is typically already sufficient for economic production. Natural hydrothermal fields are often regions of naturally enhanced permeability such as fault zones (e.g., Evans et al., 2012).

Majer et al., (2007) document examples of earthquake activity associated with EGS projects at Berlin (El Salvador), Soultz, (France), Basel (Switzerland) and the Cooper Basin (Australia). Earthquakes with magnitudes of up to 4.4 ML have been observed at the Berlin site. The largest earthquakes observed at Soultz had a magnitude of 2.7 ML, while the largest event in the Cooper Basin had a magnitude of 3.7 Mw. A series of earthquakes induced during an EGS

project in Basel, Switzerland resulted in the suspension of the project, which was ultimately abandoned almost 3 years later following further study and risk evaluation after these seismic events (Giardini, 2009). The largest event had a magnitude of 3.4 ML and was widely felt across the city by thousands of people.

More recently, a magnitude 5.5 Mw earthquake occurred near an EGS drill site at Pohang in South Korea on 15 November 2017 (Lee et al., 2019). The half-million residents of Pohang experienced violent shaking. The earthquake caused one death, injured 135 residents, displaced more than 1700 people into emergency housing, and caused more than \$75 million (US) in damage to more than 57,000 structures and more than \$300 million of total economic impact. An investigation by the Geological Society of Korea (GSK, 2019) concluded that high-pressure injection into the PX-2 borehole activated the fault that ruptured in the magnitude 5.5 Mw earthquake.

Economically efficient heat and power production from natural hydrothermal systems requires the reinjection of extracted fluids by geothermal doublet or multiplet systems (e.g., Hirschberg *et al.*, 2015). At Unterhaching in the Molasse Basin of southeast Germany, monitoring networks detected earthquakes up to 2.4 ML close to the reinjection well soon after the production phase of the plant started (Megies and Wassermann, 2014). In July 2013, a sequence of more than 340 earthquakes was induced by reservoir stimulations at a deep geothermal drilling project close to the city of St. Gallen, Switzerland (Diehl *et al.*, 2017). The largest event in the sequence had a magnitude of 3.5 ML and was felt up to 10–15 km from the epicentre.

The first TLS for managing the risk induced seismicity were originally developed for the Berlín geothermal project in El Salvador (Bommer *et al.* 2006), an area with significant background seismicity. The approach has then been used on several geothermal projects (e.g., Diehl *et al.* 2017; Häring *et al.* 2008). In some cases, the cessation of operations at a given limit did not preclude further seismicity. For example, operations were stopped during a geothermal project in the city of Basel, Switzerland (Giardini, 2009) when the red-light threshold of 2.9 ML was exceeded. However, this was still followed by several larger magnitude events that led to the project being abandoned. Similarly, the magnitude 2 red-light threshold used during the Pohang EGS project (later changed to 2.5) did not stop the damaging 5.5 Mw earthquake being triggered by the project (Lee *et al.*, 2019).

More recently, data driven, adaptive TLS (ATLS) have been suggested to address some of the limitations of the original TLS (e.g., Mignan *et al.*, 2017). These combine real-time monitoring, probabilistic forecasts, and operational adjustments. Kwiatek *et al.*, (2019) describe how an ATLS was used to control induced earthquakes during the stimulation of a 6.1-km-deep geothermal well in the metropolitan area of Helsinki, Finland. Near real-time information on induced earthquake rates, locations, magnitudes were used to vary injection rates and avoid a magnitude 2.0 Mw earthquake, or greater, the threshold set by the local authorities for stopping the project.

There are currently no specific regulations for the control or mitigation of induced seismicity associated with geothermal projects in the UK (Abesser and Walker, 2022). Control and mitigation of induced seismicity for deep geothermal operations in Cornwall (United Downs Deep Geothermal Project and Eden Geothermal Project) are based on the British Standard BS 6472-2 (BSI, 2008), which define limits for acceptable levels of ground vibrations caused by blasting and quarrying, and other local planning authority guidelines for blasting, quarrying, and mining. These thresholds are defined in terms of measured ground velocity.

5 Modelling of shales in relation to seismic activity

In this section, we discuss recent research on the geology of shale rocks in the UK and compare the geology of shales in the Bowland Basin, Lancashire with other basins with shale gas potential in the UK to answer questions 4 and 5. Key findings include:

Recent research using high quality exploration data that is available for some parts of the UK reveals localised structural and stress heterogeneity that could influence fault reactivation. This is in keeping with findings in high-hazard natural seismicity settings.

However, limited exploration data from other parts of the UK means that there are significant gaps in our knowledge of sub-surface structure of these places. When coupled with the uncertainties in predicting the magnitude, duration, timing and location of induced seismicity, it is not possible to discount the likelihood of HFIS in shale areas outside of Lancashire occurring.

It is not possible to identify all faults that could host earthquakes with magnitudes of up to 3 prior to operations, even with the best available data.

Recent research from the USA demonstrates the importance of geomechanical modelling to identify faults that are most likely to rupture during operations. This information can be used to assess risks prior to and during operations.

However, these models require accurate mapping of sub-surface faults, robust estimates of stress state, formation pore pressures and the mechanical properties of sub-surface rocks. While this information is available in a few areas with unconventional hydrocarbon potential such as the Bowland Basin, more data is needed from other basins to allow robust geomechanical models to be applied more widely.

5.1 RECENT ADVANCES IN THE MODELLING OF SHALE SUCCESSIONS IN THE UK

Shale rocks that may be prospective for oil and gas have been identified from the Carboniferous under large areas of northern England and the Midland Valley of Scotland, and the Jurassic in the Weald and Wessex basins in southern England (Figure 4).

Induced seismicity depends on the complex relationship between stress changes caused by operations, the existing faults, state of stress and the mechanical properties of the rocks themselves, e.g., coefficient of friction. Shale rocks are by their nature challenging to quantify; many of the properties relevant to seismic hazard exhibit a strong heterogeneity (e.g., lithology, stress state; Anderson et al., 2022), and this results in uncertainty in predicting properties away from regions of data coverage.

The current understanding of the characteristics of UK shale rocks is in part informed by the knowledge gained from shales in the USA that are commercially producing gas (e.g., Andrews, 2011). There are, however, some important differences between the geology of these systems that may influence shale behaviour, including geochemistry and composition of the rock, the ability to predict and correlate shale successions and the amount of geological faulting typically present. Over the past few years, several datasets acquired in the UK as part of gas exploration, including 3D seismic surveys, borehole core and down-hole geophysical log suites, have become available for scrutiny by the academic community (Appendix 1). These new data can help ground-truth exploration models and provide materials to quantify geochemical and geomechanical appraisals of shales. New geophysical data (seismic reflection and down-hole geophysics) can calibrate pre-existing 2D seismic reflection and other downhole geophysical logs, allowing for a more detailed understanding of shale geology in the UK. Shale successions, including the Bowland Shale Formation in the UK, display variation at multiple scales from the tens of metres (that may be expected to be resolved by seismic reflection exploration techniques), including large-scale cyclicity in sedimentation, through to the nanometre-scale. Typically, lab-scale analysis can help quantify variability at the tens-of-cm – nanometre-scale. However, challenges remain in the upscaling lab-scale results to the reservoir scale, resulting in less confidence in some instances in predicting and correlating properties of shale (e.g., brittle-

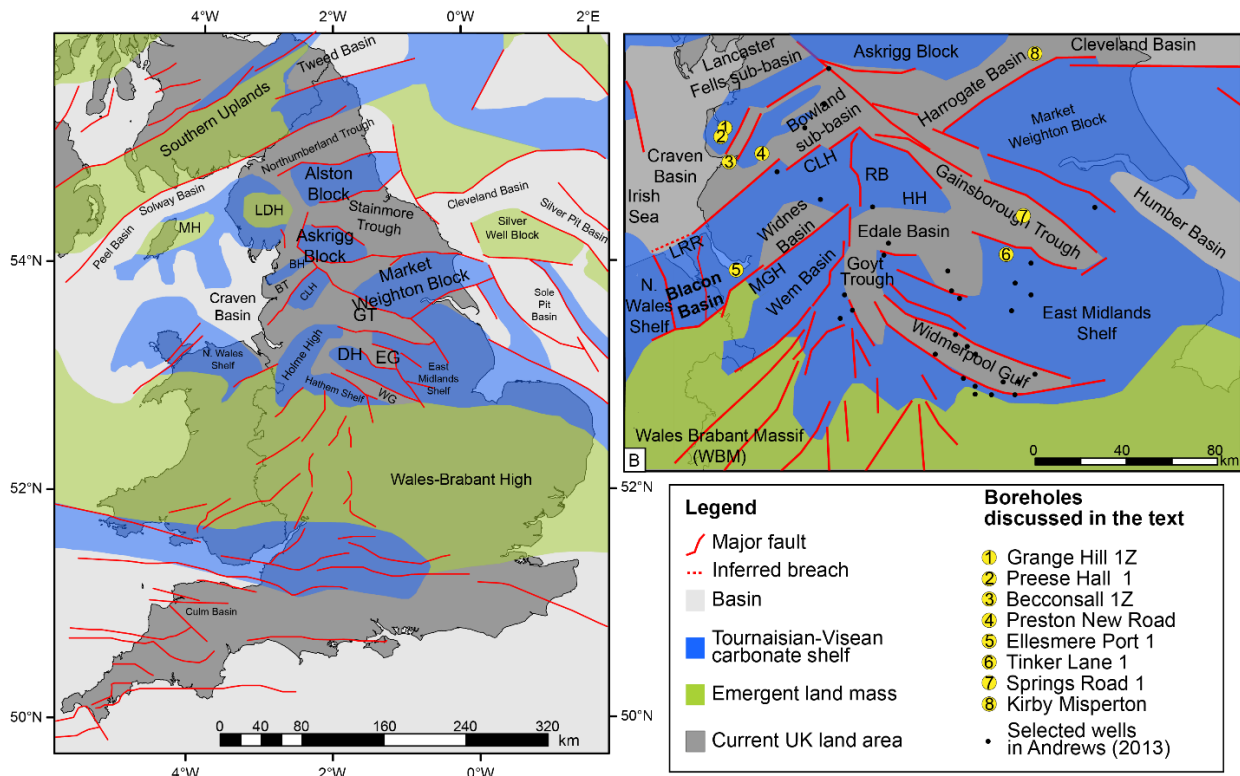


Figure 4. Carboniferous palaeogeography showing the fragmentation of the landmass at the time of deposition of the Bowland Shale Formation. BH = Bowland High; BT = Bowland Trough/Basin, CLH = Central Lancashire High; DH = Derbyshire High; EG = Edale Gulf; GT = Gainsborough Trough; LDH = Lake District High; MH = Manx High; WG = Widmerpool Gulf. (based on Waters et al., 2009; Fraser and Gawthorpe, 2003). Contains Ordnance Survey Data © Crown Copyright and database rights 2022. Ordnance Survey Licence No. 100021290 EUL.

ductile behaviour, porosity) at the seismic scale and upwards over distances in excess of a few hundred metres (e.g., Anderson et al., 2022).

Research has applied state-of-the-art interpretative techniques to recently acquired datasets, including 3D seismic and down-hole geophysics from the Fylde and north Nottinghamshire areas to improve understanding of sub-surface structure (e.g., Anderson and Underhill, 2020; Hampson et al., 2020; Anderson et al., 2022; Palci et al., 2020; Nantanoi et al., 2022). Hampson et al., (2020) indicate high levels of confidence for some of the well- to seismic reflection data correlations in the Bowland Basin, although Anderson and Underhill (2020) note challenges in interpretation, especially where data quality is sub-optimal. Some recently acquired data, however, remain unpublished or only partly described (e.g., the North Dee-15 3D seismic survey data for north Cheshire; core material for the Springs Road-1 well in north Nottinghamshire); interpretation of these data would improve knowledge of the local geology.

The mechanical properties of shales are related to their geological setting (including stratigraphy, composition, structure, in-situ and regional stress), with mineralogy impacting elastic properties (Anderson et al., 2022). The geology of UK shales is acknowledged as variable and, in some areas, e.g., Bowland Basin, Lancashire, is complex and difficult to predict beyond known data points (e.g., Waters et al., 2019; Anderson and Underhill, 2020; Palci et al., 2020). There may be value in data analysis (including petrophysical methods) as an evaluation tool in the identification of optimal exploration targets (Anderson et al., 2022). Other areas (e.g., the Gainsborough Trough that extends between Huddersfield, West Yorkshire and Welton, Lincolnshire; Palci et al., 2020, or the Cleveland Basin, North Yorkshire) have a simpler geology in terms of stratigraphy and structure and may therefore be easier to characterise. The Jurassic shales in the Wessex and Weald basins are clay rich and over large areas have not reached the gas window (Andrews, 2014; Greenhalgh, 2016), although parts of these basins produce oil and gas and they remain targets for future exploration.

The acquisition of datasets as parts of exploration programmes includes non-invasive (e.g., 3D seismic reflection) and invasive (e.g., borehole core and down-hole geophysical log data) strategies. These datasets give improved understanding of shale geology, and some important mapping exercises of shale basins, including new fault, structural and stratigraphic interpretations, and rock physics models, have been produced (e.g., Anderson and Underhill, 2020; Anderson et al., 2022). However, these are spatially restricted to a few areas in the UK, with large gaps in some areas (e.g., near Doncaster as noted by Palci et al 2020). Stress magnitude data in particular, relevant to fracture mechanics studies, is described as “limited spatially and stratigraphically” in the UK, “in particular in regions underlain by potentially prospective shale formations”, although it is possible to calculate a regional estimate of stress magnitude using the existing available data (Fellgett et al., 2018).

The acknowledgement of the need for site-specific studies and detailed evaluation to characterise potential drill sites is highlighted by several authors (e.g., Fellgett et al., 2018; Anderson and Underhill, 2020), and forms part of the existing regulatory approach. However, even with access to high-quality 3D seismic reflection data, the imaging and identification of faults may be difficult where contrasts in rock properties in the subsurface are subtle, and/or in strike-slip settings (Nantanoi et al., 2022). Additionally, the resolution of 3D seismic reflection data is variable and depends on multiple issues including land access to acquire data, complexity and scales of geological variability (see discussion in Ireland et al., 2021).

Exploration and hydraulic fracturing in structurally complex regions such as the Bowland Basin indicates that risks, including those associated with hydraulic fracturing, “cannot be mitigated through analysis of seismic data alone” (Anderson and Underhill, 2020). There remains significant uncertainty in the “risk of induced seismicity on faults that are seismically resolvable and those that are of subseismic scale” (Anderson and Underhill, 2020).

5.2 GEOMECHANICS OF HF OPERATIONS: STRESS STATE IN THE UK AND FAULT REACTIVATION POTENTIAL

For a fault to slip, the shear stress parallel to the fault plane needs to overcome the normal stress perpendicular to the fault plane that holds it locked in place. The presence of fluid in the pore spaces of the rocks on the fault plane decreases the effective normal stress, allowing the fault to slip at a lower shear stress (Hubbert and Rubey, 1959). The greater the pore pressure of the fluid, the less the clamping effect of normal stress.

The slip tendency (Morris et al., 1996) can be defined as the ratio of shear to normal stress acting on a fault. This depends on the orientation of the fault plane, the orientation and magnitude of the principal stresses, as well as the pore pressure. By studying both the geometry of faults and the contemporary stress field, it is possible to resolve the shear and normal stresses acting on known or modelled faults, and to determine which faults (or parts of faults) are most susceptible to becoming reactivated under elevated pressure conditions.

The relative orientations of a fault plane and the stress field determines if the fault is favourably oriented for failure, i.e., more likely to slip. Such favourably oriented faults may fail due to even small changes in the effective normal stress. Other fault orientations can fail but would require larger changes in effective normal stress.

Recent research from the USA and elsewhere has shown the importance of understanding faulting and stress state to better understand the expected distribution of induced seismicity from both wastewater disposal and hydraulic fracturing operations.

Lund Snee and Zoback (2020) present maps of the relative magnitude of the principal stresses and the orientation of the maximum horizontal stress (SH_{max}) that show how these change across North America. Lund Snee and Zoback (2022) present comprehensive data on stress orientation and relative magnitude in areas throughout North America where unconventional oil and gas are currently being developed. The authors suggest that this can be used both to improve operational efficiency by constraining absolute stress magnitudes and the ideal azimuth to drill horizontal wells (i.e., perpendicular to the local SH_{max} orientation) and make it possible to predict which fractures and faults are likely to be activated during hydraulic stimulation.

Hennings et al., (2021) analyse the stability of fault systems in the Delaware Basin of West Texas in relation to both wastewater injection and hydraulic fracturing. They conclude that earthquake sequences do occur on faults that are stable in normal conditions in response to elevated pore pressure from fluid injection. The authors also suggest that this approach can be used to better plan and regulate petroleum operations to avoid fault rupture. Dvory and Zoback (2021) also use data from the Delaware Basin to demonstrate that pore pressure and stress changes associated with prior oil and gas production make induced seismicity less likely. Sheng et al., (2022) carry out further detailed analysis of earthquakes in Delaware Basin, concluding that the shallow seismicity is triggered by wastewater injection.

Walsh & Zoback (2016) developed a probabilistic approach to assess fault slip potential on mapped faults that incorporates the uncertainties in different parameters such as the orientation and magnitude of the principal stresses, pore pressure, coefficient of friction, and fault orientation. The Texas Railroad Commission, who are the regulator for wastewater disposal and HF operation in Texas, require operators to carry out pre-drilling risk assessments that include the use of the Walsh & Zoback (2016) Fault Slip Potential (FSP) method for new disposal wells.

In the UK, Williams et al. (2016) used slip tendency analyses of faults in potential sandstone reservoirs for CO₂ storage in the North Sea. Healy & Hicks (2022) developed a probabilistic model of fault slip for two sites with geothermal energy potential that combines slip and dilation tendency, fracture susceptibility with response surface methodology from engineering and Monte Carlo simulations. They conclude that there are key gaps in our knowledge of the stress field, fluid pressures, and rock properties. Nantanoi et al., (2022) include measurements of stress and pore pressure in the Bowland Shale Formation to estimate fault slip potential for faults identified in the 3D seismic survey data that was acquired over the Preston New Road site and identified critically stressed faults near the PNR-1Z and PNR-2 wells. Notably, the faults that induced the largest seismic events in the Preston New Road site could not be identified in the 3D seismic survey.

However, as discussed above, estimating fault reactivation potential requires measurements of as the orientation and magnitude of the principal stresses, pore pressure, coefficient of friction, and fault orientation. Figure 5 shows measurements of the orientation of the maximum horizontal compressive stress in the UK together with the locations of wells where the magnitude of at least one of the principal stresses has been measured. The stress orientations are from the World Stress Map data release 2016 (Heidbach et al., 2018), while locations of wells where stress magnitudes have been measured are from Fellgett et al., (2018). There is generally a lack of such measurements across the UK. In particular, more detailed measurements are needed to resolve localised differences in the stress field across areas of shale gas potential.

Injection pressures used during HF operations may be such that faults do not have to be favourably oriented for failure (Shen et al., 2019; Brudzinski et al., 2019; Kettlety et al., 2020). The resulting increase in pore pressure, which decreases the effective normal stress on the fault, means that faults of many orientations may be activated. This is consistent with Segou and Parsons (2020) findings considering the pre-existing and modern stress field in California. Kettlety et al., (2020) find that the fault activated during operations in PNR-2 was more favourably oriented with respect to the local stress field than the fault activated during operations in PNR-1z. The authors suggest that this may have resulted in the larger events observed during operations in PNR-2. However, Segou and Parsons (2020) show that tectonic earthquakes also often occur on less favourable oriented faults demonstrating that even small-magnitude stress perturbations can trigger seismicity. Moreover, both dynamic earthquake triggering, where large earthquakes can trigger other events over 1,000 km away (Parsons et al., 2014) and tidal triggering suggest that the Earth's crust is always in a near-critical state of stress, with faults at the cusp of failure.

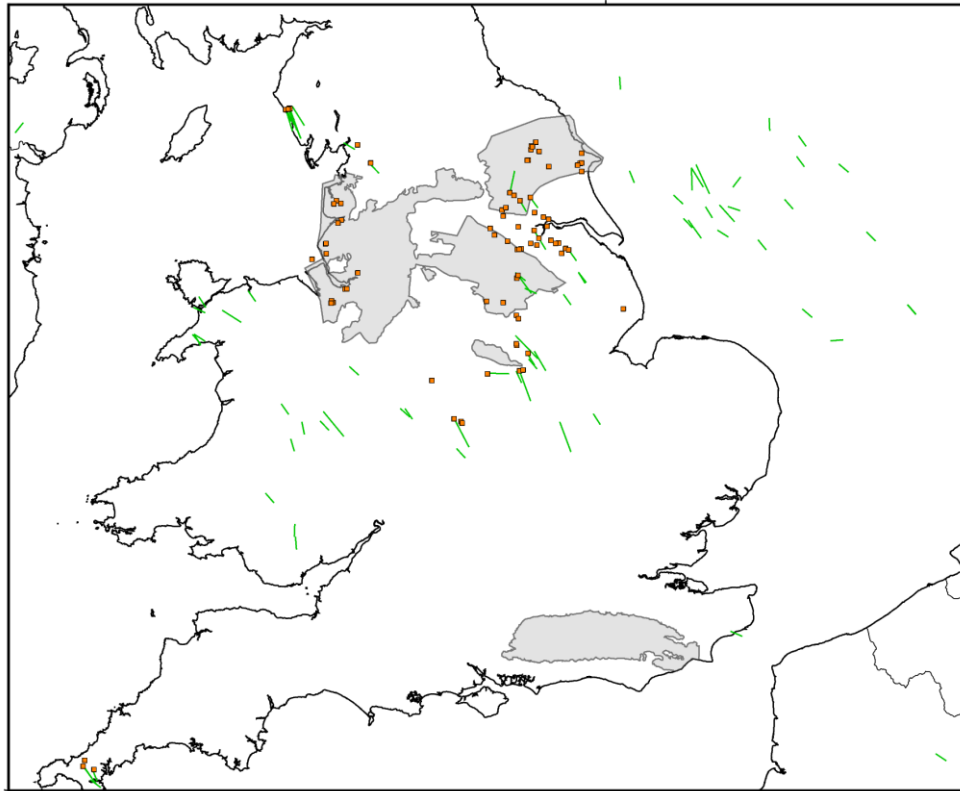


Figure 5. The orientation of the maximum horizontal compressive stress (green vectors) and locations of wells where the magnitude of at least one of the principal stresses has been measured (orange squares). Stress orientations are from the World Stress Map data release 2016 (Heidbach et al., 2018). Locations of sites where stress magnitudes have been measured are from Fellgett et al., (2018). Areas underlain by potentially prospective shale rocks are shaded grey.

5.3 SHOULD WE EXPECT HFIS IN OTHER SHALES OUTSIDE OF LANCASHIRE?

Induced earthquakes have been observed in a wide variety of geological settings and in areas where there are relatively few tectonic earthquakes (Calais et al., 2016; Ellsworth et al., 2015). In some areas, the resulting hazard from induced earthquakes due to HF operations is significantly greater than the hazard from tectonic earthquakes (Atkinson et al., 2020; Petersen et al., 2016). As a result, the low hazard from tectonic earthquakes does not guarantee that the hazard from induced seismicity will also be low.

The high-resolution spatial characterisation of shale successions in the UK is informed by a few sparsely located 3D surveys that give information on the distribution and orientation of geological faults. Outside of these areas, information describing the structure, stress and stratigraphy of the shales is typically not sufficient to give a detailed assessment of the geology. When coupled with the uncertainties in predicting the magnitude, duration, timing and location of induced seismicity, it is not possible to discount the likelihood of HFIS in shale areas outside of Lancashire, although it may be possible to quantify the risk of felt events occurring.

The shale geology in parts of the Bowland Basin is complex in terms of both stratigraphy and structure. The stratigraphy includes numerous locally and regionally developed turbidite and limestone beds, while the structure has resulted from multiple phases of burial, uplift and basin inversion and fault reactivation, associated with a diverse range of fault styles including high-angle reverse and normal faults of varying degrees of displacement associated with the development of the Ribblesdale Fold Belt (e.g., Anderson and Underhill, 2020; Pharaoh et al., 2020). For the Bowland Basin, Anderson and Underhill (2020) indicate that the identified structural complexity, including faults that are not apparent on seismic reflection data, will

influence the lateral continuity of shale horizons, and importantly the evaluation of the risk of induced seismicity on faults with a large displacement. The geology in other shale basins in the UK where studies indicate that prospective shales may be present is generally less well-known due to a smaller amount of data to describe the subsurface. Where data does exist, it indicates that these areas have also been subject to a complex depositional and structural history. Despite this, Palci et al (2020) indicate that the geological succession in the Gainsborough Trough can be mapped out with greater confidence in the south and central parts of the basin, albeit with a degree of uncertainty associated with some geological parameters including the natural fracture network.

6 Global experience of HFIS

In this section, we compare induced seismicity from hydraulic fracturing of shales in the UK, with that observed in the USA, Canada and China, to answer question 6. This includes references to some research that is important for context. Key findings include:

The rates of HF-induced seismicity in other countries where shale gas production has been ongoing for many years are observed to vary widely.

Overall, given the large number of wells with HF operations, there are relatively few published cases of HFIS.

However, in some areas the percentage of wells associated with induced earthquakes can be as high as 30%.

HF can trigger earthquakes large enough to cause structural damage. These events were not predicted in advance of operations.

The limited number of HF operations in the UK means that it is difficult to make a valid comparison of the rates of occurrence of induced seismicity with elsewhere.

Despite a large number of HF operations in wells in different basins across the USA and western Canada, only a relatively small percentage of wells can be linked to earthquake activity. Some basins show no cases of induced seismicity at all despite similar amounts of HF activity. In basins where there is induced seismicity associated with HF, it is often associated with some wells but not others.

In the USA, where around 1.8 million HF operations have been carried out in approximately 1 million wells (Gallegos and Varela, 2014), there are relatively few published cases of HF induced earthquakes that were large enough to have been widely felt (e.g., Holland, 2013; Friberg *et al.*, 2014; Skoumal *et al.*, 2015a). Skoumal *et al.* (2015b) estimated that approximately ~0.35% of ~850 unconventional wells in Ohio had induced seismicity large enough to be detected ($M > 2$). Further analysis in Ohio by Brudzinski and Kozłowska (2019) increased this to ~2.7%. In Pennsylvania and West Virginia, induced seismicity was associated with ~0.05% and ~0.3% of HF wells, respectively (Skoumal *et al.*, 2018b; Brudzinski and Kozłowska, 2019). Skoumal *et al.* (2018a) found that ~1.8% of 12,000 HF wells in Oklahoma between 2010 and 2016 were correlated with seismicity.

Atkinson *et al.* (2016) found that only ~0.3% of horizontally drilled HF wells in the Western Canada Sedimentary Basin (WCSB) were associated earthquakes with magnitudes greater than 3.0 Mw. Ghofrani and Atkinson (2020) developed a statistical model of the likelihood that horizontally fractured wells in the WCSB will trigger earthquakes with magnitudes greater than 3 and mapped how that likelihood varies spatially. Their results showed that from 14,046 HF wells with multistage hydraulic fracture treatments, the regional average probability of earthquakes with $M \geq 3$ within a 10 km radius of a HF well is 0.010 to 0.026.

However, in some areas the percentage of wells associated with induced earthquakes can be much higher. Some of the most notable examples are shown in Figure 6 and listed in Table 1. These include documented cases from the USA (Oklahoma, Texas, Ohio), Canada (Alberta, BC), the UK and China. Schultz *et al.* (2018) found that ~15% of HF wells within the Kaybob region of the Duvernay play (Alberta) were associated with induced seismicity. Kozłowska *et al.*, (2018) found that between 10% and 33% of HF wells in four ~20 × 20-km regions of Ohio had induced earthquakes. Skoumal *et al.* (2018a) finds comparable ratios in four regions in Oklahoma. Shemeta *et al.* (2019) found that 7.7% of HF wells in Oklahoma were associated with earthquakes of $ML \geq 2$, with rates as high as 19.5% in some areas. In the Bowland Shale Formation (UK), HF operations have only occurred in three wells, but these have produced events with maximum magnitudes of $M = 2.3$, 1.6 and 2.9 respectively (Clarke *et al.*, 2014; Clarke *et al.*, 2019).

The first documented example of larger earthquakes induced by HF operations was in the Horn River Basin, which lies across the border between the Northwest Territories and British

Columbia (BC), Canada, and is one of the largest shale gas plays in North America. Thirty-eight earthquakes were detected by the regional seismic monitoring network between 8/4/2009 and 13/12/2011 (BC Oil and Gas Commission, 2012). Twenty-one of the earthquakes had magnitudes of 3 ML or greater, and the largest event had a magnitude of 3.8 ML. This event was also felt by workers in the area.

The Exshaw Formation in southern Alberta has undergone limited unconventional development, however, more than 60 small earthquakes (up to 3.0 ML) were detected from December 2011 to March 2012 north of Cardston, Alberta during HF operations (Schultz *et al.*, 2015). This area had no prior documented seismic activity of comparable magnitude or frequency. The first four stimulations were aseismic whereas the following six resulted in earthquakes.

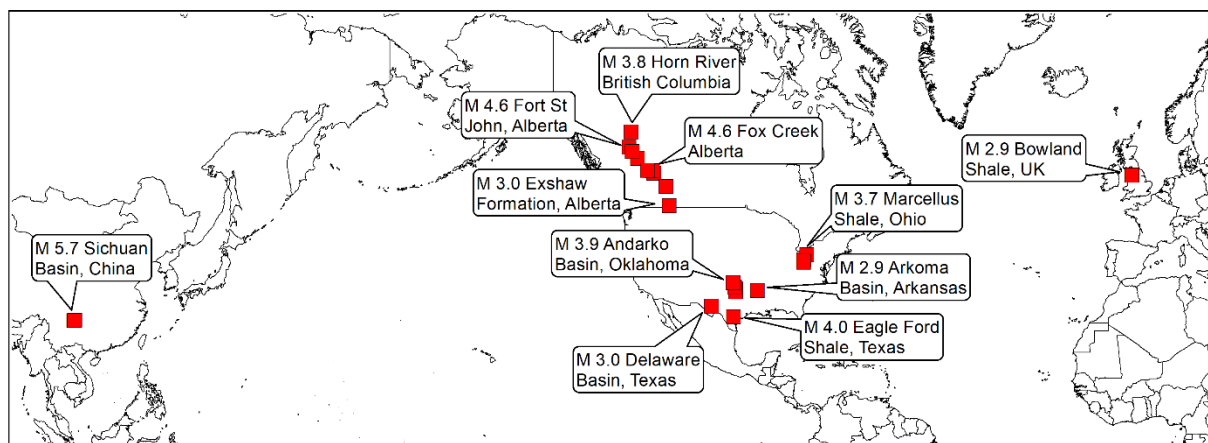


Figure 6. Global distribution of notable earthquakes induced by hydraulic fracturing (HF). This includes documented cases from the USA (Oklahoma, Texas, Ohio), Canada (Alberta, BC), the UK and China. Locations and magnitudes are from the HiQuake database (Wilson *et al.*, 2017).

The Duvernay Formation in the Alberta Basin contains vast resources of shale oil and gas. Development of the play began in 2010 and the first reported cases of induced seismicity in 2013 occurred near the town of Fox Creek (Schultz *et al.*, 2015; Schultz *et al.*, 2017). Almost 200 events with magnitudes of 2.0 ML or greater have been induced by HF operations in this basin. The largest of these was a magnitude 4.6 Mw earthquake in 2015 (Schultz *et al.*, 2017). No injuries or property damage were linked to this earthquake and the recorded ground motions were below the levels typically observed to cause damage to structures. However, the event triggered an automatic shutdown of a nearby gas plant and precautionary flaring of gas.

The Montney Formation that spans the border between BC and Alberta in western Canada is considered one of the most productive hydrocarbon plays in North America and there have been more than 7,000 HF wells completed in the formation from 2007–2020. Induced seismicity here has led to a significant change in the regional seismicity rate and around 100 events with magnitudes of 2.0 ML or greater have been induced by HF operations. The largest event was observed on 17 August 2015 in the northern Montney area with a magnitude of 4.6 Mw (Babaia Mahani *et al.*, 2017, 2019).

Oklahoma in the United States is more commonly associated with earthquakes induced by waste-water disposal, with dramatic increases in induced seismicity as a result of long-term disposal of large volumes of wastewater from both conventional and unconventional hydrocarbon production in deep boreholes (Ellsworth, 2013; Rubinstein and Mahani, 2015; Walsh and Zoback, 2016). However, induced seismicity induced by HF has also been observed in both the South Central Oklahoma Oil Province (SCOOP) and Sooner Trend (STACK) plays of the Anadarko Basin. Two of the first examples were magnitude 2.9 ML and 3.2 ML earthquakes in 2011 and 2014 in Garvin and Carter Counties, respectively (Holland, 2013; Darold *et al.*, 2014). More recently, Skoumal *et al.*, 2018a) identified 274 HF wells correlated to seismicity, with the largest a magnitude 3.5 ML event on 14 July 2015. A further 960 earthquakes with

magnitudes greater than 2 were linked to HF between 2016 and 2019, with the largest a magnitude 3.9 M_L event on 25 July 2019 in Kingfisher County.

The Utica and Marcellus Shales of the northern Appalachian Basin in the eastern United States are some of the most developed unconventional plays in the world. with more than 11,000 HF wells completed since 2009. This coincided with a significant increase in seismicity rate linked to both waste-water disposal and HF. The earliest reported case of HF-induced seismicity was in Harrison County with a magnitude 2.1 M_L earthquake in 2014 (Friberg *et al.*, 2014). Another early example was a magnitude 3.0 M_L earthquake near Poland Township (Skoumal *et al.*, 2015a). The largest recorded event linked to HF in the basin was a magnitude 3.7 M_L earthquake in Noble County, 2017.

There have been more than 19,000 HF wells completed in the Eagle Ford Shale play in South Texas along with significant increases in seismicity rates. Fasola *et al.* (2019) found that more than 85% of the seismicity in the play and 94 earthquakes with magnitudes greater than 2.0 M_L could be correlated with HF. A magnitude 4.0 M_w earthquake on 1 May 2018 earthquake is the largest HF-induced earthquake documented in the USA.

At least 7,900 HF wells have been completed in the Delaware Basin, Texas, from 2011–2019. Seismicity rates have increased significantly over the past decade, although most of the earthquake activity is thought to have been by wastewater disposal. Skoumal (2020) suggests that only 5% of seismicity was induced by HF. The largest of these was a magnitude 3.0 M_L event in May 2018.

Lei *et al.* (2017) report that since the start of hydraulic fracturing operations in December 2014, there have been rapid increases in seismicity at the Shangluo shale gas site in the Sichuan Basin, China. The authors provide evidence to suggest that earthquakes with moment magnitudes up to 4.7 M_w were caused by injection-induced fault reactivation. Lei *et al.* (2017) also suggest that the number of induced earthquakes is high in this area because of: (1) strong and brittle Pre-Triassic sedimentary rocks; (2) critical regional stress; (3) widespread existing faults; (4) insufficient top and bottom seals and/or no fracturing barrier between the shale formation and the rocks above and below.

A magnitude 5.7 M_L earthquake struck Xingwen County, Sichuan Province, China, on 16 December 2018. A few weeks later, on 3 January 2019, a magnitude 5.3 M_L earthquake occurred 8 km to the west. The largest event injured 17 people due to the collapse of nine houses and caused serious damage to more than 390 houses; it also triggered landslides and rockfalls. Lei *et al.* (2019) provide evidence to suggest that the events were induced by nearby hydraulic-fracturing operations in the Changning shale gas block at depths of 2.5-3 km. This evidence includes a strong correlation in both space and time to operations, the statistical behavior of the seismicity, and the estimated overpressure required to activate faults that are unfavourably oriented with respect to the regional stress field.

Wang *et al.*, (2022) used Sentinel-1 synthetic aperture radar data to measure surface deformation caused by the three largest earthquakes in the Changning (China) shale gas field, Sichuan, China, from 2017 to 2019, including the earthquakes on 16 December 2018 and 3 January 2019. Their results show that the earthquakes were the result of rupture on shallow faults that intersected with HF wells. These faults were in the sedimentary formations above the shale gas formations rather than basement-rooted faults. Wang *et al.*, (2022) conclude that high HF-induced seismicity rate in the Changning area is related to the relatively high strain rates in the region caused by proximity to a tectonic plate boundary.

Country	Region	Formation or Play	Age	Number of wells	Year(s)	Maximum magnitude	Significant geological factors & faulting mechanisms	Traffic Light System
Canada	Horn River Basin, BC	Muskwa Shale	DEV	11+	2009-11	Up to 3.8		No
Canada	Alberta Basin	Exshaw	DEV - CARB	~40 HF wells	2011-12	Up to 3.0	Palaeokarst adjacent to basement-rooted fault	No
Canada	Alberta Basin	Duvernay	DEV	1000 HF wells	2013-19	Up to 4.4	Basement-rooted transtensional strike-slip faults	O: 1.0 ML R: 3.0 ML
Canada	AB/BC	Montney	TRIAS	>7000 HF wells	2006-20	2.4 – 4.6	Reverse and strike-slip mechanisms	R: 4.0 ML
USA	OH, PA, VA	Marcellus & Utica	DEV - CARB	>1100 HF	2013 -	Up to 3.7	Previously unmapped linear strike-slip fault segments	O: 2.5 ML R: 3.0 ML
USA	OK; Anadarko & Arkoma Basins	SCOOP & STACK	DEV - CARB	>13000 HF wells	2013 -	Up to 3.9	Injection into dolomitic carbonates near basement. Strike-slip faulting	O: 2.5 ML R: 3.5 ML
USA	AR;	Fayetteville	CARB	>1000 HF wells	2004-09; 2010-11	Up to 2.9	Activation of strike-slip basement faulting.	No.
USA	TX;	Eagle Ford	CRET	>19000 HF		Up to 4.0	Normal faulting	No
USA	TX, NM: Delaware Basin	Wolfcamp & Bone Spring	PERM	>7900 HF wells (TX)	2010 -	Up to 3.0		No
China	South Sichuan Basin	Wufeng - Longmaxi	ORD - SIL	>500 HF wells	2014 -	Up to 5.7	Reverse or strike slip movement in dolomitic strata between target and basement	No
UK	LANC	Bowland	CARB	2 HF wells	2011; 2018-19	2.3; 1.6, 2.9	Fluid injection directly into fault	O: 0.0 ML R: 0.5 ML

Table 1. Summary of documented cases of hydraulic fracturing induced seismicity reviewed by Schultz *et al.* 2020a. CRET Cretaceous, TRIAS Triassic, PERM Permian, CARB Carboniferous, DEV Devonian; SIL Silurian; ORD Ordovician. HF Hydraulic fracturing; WWI wastewater injection. O: orange; R: red.

7 Conclusions

This report draws on scientific advances published since the pause on shale gas extraction in England was implemented in 2019. We have included peer-reviewed research published in scientific journals, together with relevant technical reports from regulators and public bodies. Research pre-dating 2019 is included where it is needed to put more recent work in context.

The following conclusions are relevant to questions 1 and 2 from the terms of reference, which ask about “new techniques” to “reduce the risk of seismic events” and “if they would be suitable for use in the UK”.

Earthquake forecasting remains a scientific challenge for the geoscience community. Maximum expected magnitude, the time scales for the occurrence of large-magnitude earthquakes and the variability of earthquake sequences across the world are all areas of ongoing research. The complexity of this challenge is partly related, among other factors, to the relatively short historic records when compared with the longer recurrence time for large earthquakes, the current state of modern seismic monitoring and significant existing knowledge gaps about earthquake processes. These challenges and issues are shared in natural and induced earthquakes alike.

The estimation of maximum magnitudes before and during HF operations remains challenging. Methods that relate injected volume to the maximum magnitude or numbers of events show some promise, but when applied to the rich datasets from operations at PNR, provide estimates that are lower than the maximum observed magnitude. For faults that extend outside the immediate hydraulically fractured zone, the maximum magnitude will be controlled by local geology and tectonics, not only by operational parameters, such as the amount of injected fluid.

The development of statistical and physics-based forecast models over the last decade for tectonic (natural) earthquakes aims to support decision-making and raise awareness of future hazards. These forecast models provide time-dependent probabilistic estimations for the occurrence of earthquakes above a magnitude threshold within a given time (and space) window of interest. These forecasts have also been adapted for induced seismicity by including, either implicitly or explicitly, operational parameters such as injection rate. Such models may incorporate the maximum magnitude for tectonic earthquakes at the site of interest, and their generic parameterization can be calibrated using well-specific information.

However, these forecast models are data intensive, and their real-time implementation requires detailed earthquake catalogues. Recent technological advances based on machine-learning algorithms promise to deliver high-quality, high-resolution earthquake datasets to support forecasting models in operational settings. The latest machine learning algorithms can detect and locate many times more earthquakes than conventional approaches, even using a fraction of the available seismic stations. The retrospective implementation of ML techniques in the USA has allowed high-resolution mapping of previously unknown fault structures in areas of induced seismicity over a decade of operations that could inform future mitigation actions.

Probabilistic methods, like those used to quantify risks from tectonic earthquakes can be used to assess risks of induced seismicity, including HFIS. However, there are important differences between how tectonic and induced seismicity evolves in space and time. Recent studies have shown how earthquake statistics can be used to address this problem, but further work is needed to develop these models and incorporate them in risk assessments.

Existing risk mitigation techniques, such as traffic light systems, remain important tools. However, red-light thresholds should be chosen to ensure that the probability of the scenario to be avoided, e.g., disturbing or damaging ground motions, is at an acceptable level. Amber light thresholds should be chosen as much as two magnitude units below the red-light threshold. Recent advances in risk assessments in hydraulic fracturing operations that consider the nuisance and damage potential from earthquake ground shaking should be used to determine these thresholds and should incorporate the possibility of both magnitude jumps and trailing events that occur after operations are stopped or paused. Thresholds that relate to specific risk

targets should make the decision-making process more transparent. These may vary geographically depending on levels of risk tolerance.

A red-light event usually results in the complete cessation of operations in a well, rather than a brief pause, because of the increased risk of larger magnitude events. There should also be sufficient space between the amber and red-light thresholds to ensure that operators have a sufficient opportunity to enact mitigation strategies and reduce the possibility of events jumping from yellow to red.

The following conclusions are relevant to question 3 from the terms of reference, which asks “how does the seismicity caused by fracturing compare to other forms of underground energy production” the different thresholds for activity” used in other industries.

Induced seismicity has been observed in other industries related to underground energy production both in the UK and elsewhere. In the absence of a seismic building code in the UK, consistent risk targets, i.e., scenarios to be avoided, could be considered for all energy related industries that present a risk of induced earthquakes. This would allow greater transparency and would help improve public perception of the risks. Useful insights may be gained from regulatory approaches used elsewhere for the mitigation of induced seismicity associated with other energy technologies and industries.

The following conclusions are relevant to questions 4 and 5 from the terms of reference, which ask “modelling of shale has improved in the period since 2019”, “do these improvements mean we could be confident about the modelling of seismic events”, and “are there other sites, outside of Lancashire, which might be at a substantially lower risk of seismic activity”.

It remains challenging to identify and characterize faults that could host seismic events of magnitudes up to 3.0 even when using 3-D seismic reflection survey ahead of operations. These may only be revealed by seismicity recorded as HF operations are ongoing. This was the case during HF operations at PNR where microseismicity recorded by a downhole array was aligned on the activated fault structure.

Recent research from the USA demonstrates the importance of geomechanical modelling to identify faults that are most likely to rupture during operations. This information can be used to assess risks prior to and during operations. However, these models require accurate mapping of sub-surface faults, robust estimates of stress state, and knowledge of formation pore pressures and the mechanical properties of sub-surface rocks. While this information is available in a few areas, more data is needed in other basins in the UK with unconventional hydrocarbon potential to apply this more widely.

The stratigraphy and structural geology of the Bowland Basin is complex because of multiple phases of deformation through geological history. Different fault styles are observed on a wide variety of scales, and combined with geological variability, leads to shale formations that are typically laterally discontinuous, particularly at scales of less than 1 km. There is less data available from other basins in the UK with unconventional hydrocarbon potential, but the existing data suggests that these areas share a complex depositional and structural history, with the possible exception of the Gainsborough Trough and Cleveland Basin.

The following conclusions are relevant to question 6 from the terms of reference, which asks “how does seismicity from fracturing in the UK compare to other countries”.

In natural seismicity settings scientists accept that only one in ten earthquakes is followed by a larger magnitude earthquake. Research in induced seismicity settings in the USA and Canada suggests that on average around 1% of HF wells can be linked to earthquakes with magnitudes of 3 or greater, although in some areas of the USA and Canada the percentage of wells associated with induced earthquakes is much higher (>30%).

HF can trigger earthquakes large enough to cause structural damage. These events were not predicted in advance of operations.

The limited number of HF operations in the UK (three exploratory wells), makes it impossible to determine with statistical significance the rates of occurrence of induced seismicity from HF operations using solely national data, underlying the importance of international collaboration and knowledge exchange in monitoring and operational practices.

Data and Resources

The original microseismicity catalogues and pumping data from operations at Preston New Road are available from the North Sea Transition Authority (ex-Oil and Gas Authority) and available at <https://www.nstauthority.co.uk/exploration-production/onshore/onshore-reports-and-data/>.

Homogenised catalogues of microseismicity and pumping data from the PNR-1z and PNR-2 injection wells used by Mancini et al., (2021) in Figure 2 are available at the National Geoscience Data Centre, <https://doi.org/10.5285/856fc9f4-bea8-490f-b709-92549d692da4>. This data set is available under Open Government Licence.

The combined catalogue of microseismic events recorded during Cuadrilla's Preston New Road hydraulic fracturing operations containing all the seismic magnitudes used in Figure 3 was prepared by Kettleby, T. & Butcher, A. (2022) and is available at the National Geoscience Data Centre, <https://doi.org/10.5285/709cbc2f-af5c-4d09-a4ea-6deb5aa8c5d8>. This data set is available under Open Government Licence.

Stress orientations used in Figure 5 are from the World Stress Map data release 2016 (Heidbach et al., 2018) and are available at <https://www.world-stress-map.org/download>. The data are publicly available.

Locations of sites where stress magnitudes have been measured used in Figure 5 are from Fellgett et al., (2018).

The UK Shale Prospective Areas data used in Figure 6 are available from the North Sea Transition Authority, <https://www.nstauthority.co.uk/exploration-production/onshore>. This data set is available under Open Government Licence.

The Human-Induced Earthquake Database (Wilson et al., 2017) used in Figure 6 is an open-access database available at <https://www.inducedearthquakes.org>.

Information regarding downhole geophysical log data and 2D and 3D seismic surveys is available from the UK Onshore Geophysical Library: <https://ukogl.org.uk/>

Earthquake and geological map and borehole information is available from the British Geological Survey GeolIndex: <https://www.bgs.ac.uk/map-viewers/geology-of-britain-viewer/>

Glossary and acronyms

Borehole – Any hole drilled or dug into the sub-surface for the purpose of extracting or investigating the material at that particular point. Commonly cylindrical, the length of the hole will always be several orders of magnitude greater than its width or diameter. Boreholes include any drilled onshore and offshore, for any purpose and to any depth. As opposed to wells, which are typically used for the extraction of natural resources, the term ‘borehole’ is more often used to describe a hole that was drilled for scientific purposes.

Earthquake – Ground shaking caused by the sudden release of energy that results from the movement or slip on a fault in the Earth’s sub-surface.

EGS – Enhanced Geothermal Systems are geothermal reservoirs enabled for economic utilization of low permeability conductive rocks by creating fluid connectivity in initially low-permeability rocks through hydraulic, thermal, or chemical stimulation (Huenges, 2016).

Epicentre – the location of the point of initiation of an earthquake, projected to the Earth’s surface.

ETAS: Epidemic Type Aftershock Sequence model of the spatial and temporal evolution of seismicity based on earthquake statistics presented in Ogata (1988).

Fractures – A planar discontinuity in a medium. Fractures that lack shear offset are called joints. Fractures can accommodate fluid-flow along the spaces between the rocks. In the context of HF-induced seismicity, these are intentionally stimulated by injection of fluid for resource production.

Fault – Discontinuities in a volume of rock where there has been displacement caused by relative movement of the rock-mass. Often simplified planar geometries are used to approximate the fault, although individual faults may in fact be much more complex. Faults are classified using the angle of the fault with respect to the surface (known as the dip) and the direction of slip along the fault.

GMPEs – Ground Motion Prediction Equations estimate the ground motion that may occur at a site when exposed to an earthquake of a certain magnitude taking place nearby (Douglas and Edwards 2016).

Geothermal doublet (multiplet) – A system of exploiting geothermal energy made up of two wells: an injection well and a production well. Warm water is pumped up the production well to the surface where it is used and re-injected at depth.

Horizontal Well – A well that is drilled vertically, until reaching the target formation where it is deviated into a horizontal orientation. The section where the transition from vertical to horizontal occurs is called the “heel” and the end of the horizontal portion is called the “toe”. Typically, horizontal sections are up to 2 km in length.

Hydraulic fracturing (HF); “fracking” – the methodology to prepare impermeable shale for production of shale gas. During hydraulic fracturing, a mixture of water, chemicals and sand is pumped down a borehole at high pressure. The water pressure opens up cracks in the rock and the sand grains lodge into the spaces to keep them open, allowing the released gas to flow out of the rocks and travel back up the borehole where it is captured. The hydraulic fracturing technique is not new; it has been used for over 50 years to improve recovery of conventional oil and gas.

Hypocentre (also known as the focus) – The location (in the subsurface) where an earthquake rupture initiates.

Induced seismicity (or HFIS) – Hydraulic Fracturing Induced Seismicity A type of earthquake activity that is caused or accelerated by human activities. Sometimes these earthquakes are distinguished into either triggered or induced, depending on the degree of human influence. In this paper we make no distinction and refer to both types as induced

Kerogen – hydrocarbon component of shale that generates oil or gas when heated.

Local Magnitude (M_L) – The original earthquake magnitude scale developed by Richter (1935) based on observations of earthquakes in Southern California. Although the scale is only strictly applicable there, it has been used all around the world.

Magnitude – A measure of the amount of energy released during an earthquake. Magnitude is usually estimated from measured records of ground motion with specific corrections for distance. Most magnitude scales are logarithmic so that each whole number increase in magnitude represents a tenfold increase in measured amplitude and about 32 times the energy released.

Microseismicity – Earthquakes with magnitudes of less than 2.0 that are usually too small to be felt (e.g., Vilarrasa et al., 2019).

Mitigation – Procedures enacted by the HF operator to reduce the likelihood and impacts of induced seismicity.

Operator – The company who owns the HF pad and is responsible for completion.

Play – A term used to denote the extent of a target formation (or a package of formations) exploited by HF.

PNR – Preston New Road: one of the sites in the UK where HF took place (with Cuadrilla Resources as the operator) and induced seismicity was recorded (see Appendix 1).

Porosity – The proportion of filled space to empty space in a rock.

Regulator – The institution responsible for the oversight of responsible operator development.

Shale – is a fine-grained, sedimentary rock formed as a result of the compaction of clay, silt, mud and organic matter over time and is usually considered equivalent to mudstone. Shales were deposited in ancient seas, river deltas, lakes and lagoons and are one of the most abundant sedimentary rock types, found at both the Earth's surface and deep underground. A shale gas reservoir would be expected to be dominantly shale in composition but many include beds or units of limestone or sandstone at varying scales.

Shale gas (=unconventional gas) – is natural gas found in shale deposits, where it is trapped in microscopic or sub-microscopic pores. This natural gas is a mixture of naturally occurring hydrocarbon gases produced from the decomposition of organic matter (plant and animal remains). Typically, shale gas consists of 70 to 90 per cent methane (CH_4), the main hydrocarbon target for exploration companies. This is the gas used for generating electricity and for domestic heating and cooking.

Shale oil (=unconventional oil) – is the result of the decomposition of kerogen in shale when the organic matter has not been exposed to same temperatures and pressures as is the case for shale gas (lower maturity than shale gas).

TLS (=Traffic Light System) – Guidance to manage onshore induced seismicity, issued by BEIS (<https://www.gov.uk/government/publications/traffic-light-monitoring-system-shale-gas-and-fracking>). Operators are required to carry out seismic monitoring whereby injection can proceed if the recorded magnitude (M) < 0.0; injection can proceed with caution if M is 0.0–0.5, possibly at reduced rates with more intensive monitoring; when $M \geq 0.5$, the operator must suspend injection, reduce pressure and monitor seismicity and ground motion for any further events before potentially resuming.

Turbidite – A geological formation deposited by a turbidity current, which is a rapid, downslope, high density, sediment-laden current. They can be triggered by geological disturbances like earthquakes at the time of deposition.

Well – In petroleum geology, a well is considered a borehole that is completed for the production of a resource (oil or gas) as opposed to a 'borehole' which is drilled mainly for scientific purposes.

References

- Abesser, C, Busby, JP, Pharaoh, TC, Bloodworth, AJ & Ward, RS. (2020). Unlocking the potential of geothermal energy in the UK. BGS Open Report OR/20/049, 22 pp.
- Abesser, C & Walker, A. (2022). Geothermal energy. UK Parliament POST brief No. 46. <https://post.parliament.uk/research-briefings/post-pb-0046/>.
- Allis, R.G. (1982). Mechanism of induced seismicity at the Geysers Geothermal Reservoir, California. *Geophysical Research Letters* **9**, 629–632. <https://doi.org/10.1029/gl009i006p00629>.
- Anderson, I. & Underhill, J.R. (2020). Structural constraints on Lower Carboniferous shale gas exploration in the Craven Basin, NW England. *Petroleum Geoscience*, **26**, 303–324. <https://doi.org/10.1144/petgeo2019-125>.
- Anderson, I., Ma, J., Wu, X., Stow, D. & Griffiths, D. (2022). Bowland Shale well placement strategy – Part 2: Fracture simulations using a 3D geomechanical model and implications for stratigraphic and spatial horizontal well locations. *Energy Geoscience*, **3**, 235–254. <https://doi.org/10.1016/j.engeos.2022.03.004>.
- Andrews, I.J. (2014). The Jurassic shales of the Weald Basin: geology and shale oil and shale gas resource estimation. British Geological Survey Report for Department of Energy and Climate Change, London, UK. https://www.nstauthority.co.uk/media/2774/bgs_decc_jurassicwealdshale_study_2014_main_report_low_res.pdf.
- Atkinson, G.M., (2015). Ground-Motion Prediction Equation for Small-to-Moderate Events at Short Hypocentral Distances, with Application to Induced-Seismicity Hazards. *Bulletin of the Seismological Society of America*, **105**, 981–992. <https://doi.org/10.1785/0120140142>.
- Atkinson, G.M., Eaton, D.W., Ghofrani, H., Walker, D., Cheadle, B., Schultz, R., Shcherbakov, R., Tiampo, K., Gu, J., Harrington, R.M., Liu, Y., van der Baan, M. & Kao, H., (2016). Hydraulic Fracturing and Seismicity in the Western Canada Sedimentary Basin. *Seismological Research Letters*, **87**(3), 631-647. <https://doi.org/10.1785/0220150263>.
- Atkinson, G. M., Eaton, D. W., & Igonin, N. (2020). Developments in understanding seismicity triggered by hydraulic fracturing. *Nature Reviews Earth & Environment*, **1**(5), 264–277. <https://doi.org/10.1038/s43017-020-0049-7>.
- Babaie Mahani, A., Schultz, R., Kao H., Walker, D., Johnson, J. & Salas, C. (2017). Fluid injection and seismic activity in the northern Montney Play, British Columbia, Canada, with special reference to the 17 August 2015 Mw 4.6 induced earthquake. *Bulletin of the Seismological Society of America*, **107**(2), 542–552.
- Babaie Mahani, A., Kao, H., Atkinson, G. M., Assatourians, K., Addo, K., & Liu, Y. (2019). Ground motion characteristics of the 30 November 2018 injection-induced earthquake sequence in northeast British Columbia, Canada. *Seismological Research Letters*, **90**(4), 1457–1467. <https://doi.org/10.1785/0220190127>
- Baisch, S., Koch, C., & Muntendam-Bos, A. (2019). Traffic light systems: To what extent can induced seismicity be controlled? *Seismological Research Letters*, **90**(3), 1145–1154. <https://doi.org/10.1785/0220180337>.
- Baker, J., Bradley, B., Stafford, P., (2021). Seismic Hazard and Risk Analysis. Cambridge University Press, Cambridge, 582pp. <https://doi.org/10.1017/9781108425056>.
- Bao, X., & Eaton, D. W. (2016). Fault activation by hydraulic fracturing in western Canada. *Science*, **354**, 1406–1409. <https://doi.org/10.1126/science.aag2583>.
- BC Oil and Gas Commission (2012). *Investigation of observed seismicity in the Horn River basin* (Technical report) BC Oil and Gas Comm., Victoria, B. C., Canada. www.bccogc.ca/node/8046/download.

- Beroza, G.C., Segou, M. & Mostafa Mousavi, S. Machine learning and earthquake forecasting—next steps. *Nature Communications*, **12**, 4761 (2021). <https://doi.org/10.1038/s41467-021-24952-6>.
- Bischoff, M., Cete, A., Fritschen, R. & Meier, T. (2010). Coal Mining Induced Seismicity in the Ruhr Area, Germany. *Pure and Applied Geophysics*, **167**, 63–75. <https://doi.org/10.1007/s00024-009-0001-8>.
- Bishop, I., Styles, P. & Allen, M. (1993). Mining-induced seismicity in the Nottinghamshire Coalfield. *Quarterly Journal of Engineering Geology and Hydrogeology*, **26**, 253–279. <https://doi.org/10.1144/GSL.QJEGH.1993.026.004.03>.
- Bommer, J.J., Crowley, H., Pinho, R., (2015). A risk-mitigation approach to the management of induced seismicity. *Journal of Seismology* **19**, 623–646. <https://doi.org/10.1007/s10950-015-9478-z>.
- Bourne, S.J., Oates, S., Van Elk, J. & Doornhof, D. (2014). A seismological model for earthquakes induced by fluid extraction from a subsurface reservoir. *Journal of Geophysical Research*, **119**, 8991–9015.
- Bourne, S.J., Oates, S.J. & Van Elk, J. (2018). The exponential rise of induced seismicity with increasing stress levels in the Groningen gas field and its implications for controlling seismic risk. *Geophysical Journal International*, **213**(3), 1693–1700.
- Browitt, C.W.A., Turbitt, T. & Morgan, S.N. (1985) 3. Investigation of British earthquakes using the national monitoring network of the British Geological Survey, *Earthquake Engineering in Britain*, pp. 33–47. <https://doi.org/10.1680/eeib.02463.0004>.
- Brudzinski, M. R., & Kozłowska, M. (2019). Seismicity induced by hydraulic fracturing and wastewater disposal in the Appalachian Basin, USA: A review. *Acta Geophysica*, **67**(1), 351–364. <https://doi.org/10.1007/s11600-019-00249-7>
- BSI, (2008). Guide to evaluation of human exposure to vibration in buildings - Part 2: Blast-induced vibration. BS 6472-2: 2008, British Standards Institution, London. <https://doi.org/10.3403/30113307>.
- Calais, E., Camelbeeck, T., Stein, S., Liu, M., & Craig, T. J. (2016). A new paradigm for large earthquakes in stable continental plate interiors. *Geophysical Research Letters*, **43**, 10,621–10,637. <https://doi.org/10.1002/2016GL070815>.
- Clarke, H., Eisner, L., Styles, P., & Turner, P. (2014). Felt seismicity associated with shale gas hydraulic fracturing: The first documented example in Europe. *Geophysical Research Letters*, **41**, 8308–8314. <https://doi.org/10.1002/2014GL062047>
- Clarke, H., Turner, P., Bustin, R.M., Riley, N., Besly, B., (2018). Shale gas resources of the Bowland Basin, NW England: a holistic study. *Petroleum Geoscience*, **24**, 287–322. <https://doi.org/10.1144/petgeo2017-066>.
- Clarke, H., Verdon, J.P., Kettlety, T., Baird, A. F., & Kendall, J. M. (2019). Real-time imaging, forecasting, and management of human-induced seismicity at Preston New Road, Lancashire, England. *Seismological Research Letters*, **90**(5), 1902-1915. <https://doi.org/10.1785/0220190110>.
- Cook, N.G.W., 1976. Seismicity associated with mining. *Engineering Geology*, **10**, 99–122. [https://doi.org/10.1016/0013-7952\(76\)90015-6](https://doi.org/10.1016/0013-7952(76)90015-6).
- Corlett, H., Schultz, R., Branscombe, P., Hauck, T., Haug, K., MacCormack, K., & Shipman, T. (2018). Subsurface faults inferred from reflection seismic, earthquakes, and sedimentological relationships: Implications for induced seismicity in Alberta, Canada. *Marine and Petroleum Geology*, **93**, 135–144. <https://doi.org/10.1016/j.marpetgeo.2018.03.008>.
- Cremen, G., Werner, M.J. & Baptie, B. (2019). A New Procedure for Evaluating Ground-Motion Models, with Application to Hydraulic-Fracture-Induced Seismicity in the United Kingdom. *Bulletin of the Seismological Society of America*, **110**, 2380–2397, <https://doi.org/10.1785/0120190238>.

- Cremer, G. & Werner, M.J. (2020). A novel approach to assessing nuisance risk from seismicity induced by UK shale gas development, with implications for future policy design. *Natural Hazards and Earth System Sciences*, **20**, 2701–2719. <https://doi.org/10.5194/nhess-20-2701-2020>.
- Darold, A., Holland, A. A., Chen, C., & Youngblood, A. (2014). *Preliminary analysis of seismicity near Eagleton 1–29, Carter County*. Oklahoma Geological Survey Open File Report OF2-2014, Oklahoma Geological Survey.
- Davies, R., Foulger, G., Bindley, A. & Styles, P. (2013). Induced seismicity and hydraulic fracturing for the recovery of hydrocarbons. *Marine and Petroleum Geology*, **45**, 171–185. <http://dx.doi.org/10.1016/j.marpetgeo.2013.03.016>.
- Davison, C. (1919). II.—On the Stafford Earthquakes of January 14–15, 1916, and on the Relations between the Twin-Earthquakes of the Midland Counties. *Geological Magazine* **6**, 302–312. <https://doi.org/10.1017/s0016756800204275>.
- Dempsey, D. & Suckale, J. (2017). Physics-based forecasting of induced seismicity at Groningen gas field, the Netherlands. *Geophysical Research Letters*, **44**, 7773–7782.
- Department for Business, Energy & Industrial Strategy (2013). Regulatory Roadmap: Onshore oil and gas exploration in the UK regulation and best practice. <https://www.gov.uk/government/publications/regulatory-roadmap-onshore-oil-and-gas-exploration-in-the-uk-regulation-and-best-practice>.
- Diehl, T., Kraft, T., Kissling, E. & Wiemer, S. (2017). The induced earthquake sequence related to the St. Gallen deep geothermal project (Switzerland): Fault reactivation and fluid interactions imaged by microseismicity. *Journal of Geophysical Research: Solid Earth*, **122**, 7272–7290. <https://doi.org/10.1002/2017jb014473>.
- Douglas, J. & Edwards, B. (2016). Recent and future developments in earthquake ground motion estimation. *Earth Science Reviews*, **160**, 203–219. <https://doi.org/10.1016/j.earscirev.2016.07.005>.
- Dvory, N.Z. & Zoback, M.D. (2021). Prior oil and gas production can limit the occurrence of injection-induced seismicity: A case study in the Delaware Basin of western Texas and southeastern New Mexico, USA. *Geology*, **49** (10), 1198–1203. <https://doi.org/10.1130/G49015.1>.
- Eaton, D. W., & Schultz, R. (2018). Increased likelihood of induced seismicity in highly overpressured shale formations. *Geophysical Journal International*, **214**(1), 751–757. <https://doi.org/10.1093/gji/ggy167>.
- Eaton, D. W., Igonin, N., Poulin, A., Weir, R., Zhang, H., Pellegrino, S., & Rodriguez, G. (2018). Induced Seismicity Characterization during Hydraulic-Fracture Monitoring with a Shallow-Wellbore Geophone Array and Broadband Sensors. *Seismological Research Letters*, **89**(5), 1641–1651. <https://doi.org/10.1785/0220180055>
- Edwards, B., Crowley, H., Pinho, R. & Bommer, J.J. (2021). Seismic Hazard and Risk Due to Induced Earthquakes at a Shale Gas Site. *Bulletin of the Seismological Society of America*, **111**(2), 875–897. <https://doi.org/10.1785/0120200234>.
- Ellsworth, W. L. (2013). Injection-induced earthquakes. *Science*, **341**(6142), 1225942. <https://doi.org/10.1126/science.1225942>
- Ellsworth, W. L., Llenos, A. L., McGarr, A. F., Michael, A. J., Rubinstein, J. L., Mueller, C. S., Petersen, M. D., & Calais, E. (2015). Increasing seismicity in the US midcontinent: Implications for earthquake hazard. *The Leading Edge*, **34**(6), 618–626. <https://doi.org/10.1190/tle34060618.1>
- Ellsworth, W. L., Giardini, D., Townend, J., Ge, S., & Shimamoto, T. (2019). Triggering of the Pohang, Korea, earthquake (Mw 5.5) by enhanced geothermal system stimulation. *Seismological Research Letters*, **90**(5), 1844–1858. <https://doi.org/10.1785/0220190102>.

- Evans, K.F., Zappone, A., Kraft, T., Deichmann, N. & Moia, F. (2012). A survey of the induced seismic responses to fluid injection in geothermal and CO₂ reservoirs in Europe. *Geothermics* **41**, 30–54. <https://doi.org/10.1016/j.geothermics.2011.08.002>.
- Eyre, T. S., Eaton, D. W., Zecevic, M., D'Amico, D., & Kolos, D. (2019). Microseismicity reveals fault activation before Mw 4.1 hydraulic-fracturing induced earthquake. *Geophysical Journal International*, **218**(1), 534–546. <https://doi.org/10.1093/gji/ggz168>
- Farahbod, A. M., Kao, H., Cassidy, J. F., & Walker, D. (2015). How did hydraulic-fracturing operations in the Horn River Basin change seismicity patterns in northeastern British Columbia, Canada? *The Leading Edge*, **34**(6), 658–663. <https://doi.org/10.1190/tle34060658.1>
- Fasola, S. L., Brudzinski, M. R., Skoumal, R. J., Langenkamp, T., Currie, B. S., & Smart, K. J. (2019). Hydraulic fracture injection strategy influences the probability of earthquakes in the Eagle Ford shale play of South Texas. *Geophysical Research Letters*, **46**, 12,958–12,967. <https://doi.org/10.1029/2019GL085167>
- Fellgett, M.W, Kingdon, A., Williams, J.D.O. and Gent, C.M.A (2018). Stress magnitudes across UK regions: New analysis and legacy data across potentially prospective unconventional resource areas. *Marine and Petroleum Geology*, **97**, 24–31. <https://doi.org/10.1016/j.marpetgeo.2018.06.016>.
- Foulger, G.R., Wilson, M. P., Gluyas, J. G., Julian, B. R., & Davies, R. J. (2018). Global review of human-induced earthquakes. *Earth Sci. Rev.* **178**, 438–514 <https://doi.org/10.1016/j.earscirev.2017.07.008>.
- Fraser, A. J. & Gawthorpe, R. L. (2003). An Atlas of Carboniferous Basin Evolution in Northern England. *Geological Society of London, Memoirs*, **28**. <https://doi.org/10.1144/GSL.MEM.2003.028>.
- Friberg, P.A., Besana-Ostman, G.M. & Dricker, I. (2014). Characterization of an earthquake sequence triggered by hydraulic fracturing in Harrison County, Ohio. *Seismological Research Letters*, **85**(6), 1295–1307.
- Gallegos, T. J. & Varela, B.A. (2014). *Trends in hydraulic fracturing distributions and treatment fluids, additives, proppants, and water volumes applied to wells drilled in the United States from 1947 through 2010: Data analysis and comparison to the literature*. U.S. Geological Survey Science Investigation Report 2014-5131.
- Ghofrani, H., & Atkinson, G. M. (2020). Activation rate of seismicity for hydraulic fracture wells in the Western Canada Sedimentary Basin. *Bulletin of the Seismological Society of America*. <https://doi.org/10.1785/0120200002>
- Giardini, D. (2009). Geothermal quake risks must be faced. *Nature*, **462**, 848–849. <https://dx.doi.org/10.1038/462848a>.
- Greenhalgh, E. (2016). The Jurassic shales of the Wessex Area: geology and shale oil and shale gas resource estimation, British Geological Survey Report for the Oil and Gas Authority, London, UK. https://www.nstauthority.co.uk/media/2785/bgs_oga_2016_wessex_main_report.pdf.
- Grigoli, F., Cesca, S., Priolo, E., Rinaldi, A.P., Clinton, J.F., Stabile, T.A., Dost, B., Fernandez, M.G., Wiemer, S. & Dahm, T. (2017). Current challenges in monitoring, discrimination, and management of induced seismicity related to underground industrial activities: a European perspective. *Reviews of Geophysics*, **55**, 310–340. [https://dx.doi.org/10.1016/s0016-2361\(98\)80024-0](https://dx.doi.org/10.1016/s0016-2361(98)80024-0)
- Gutenberg, B. & Richter, C.F. (1954). *Seismicity of the Earth and Associated Phenomena*, 2nd ed., Princeton University Press.
- Hallo, M., Oprsal, I., Eisner L. & Ali M.Y. (2014). Prediction of magnitude of the largest potentially induced seismic event. *Journal of Seismology*, **18**, 421–431.
- Hampson, M., Martin, H., Craddock, L., Wood, T. & Rylands, E. (2020). The Elswick Field, Bowland Basin, UK Onshore, in: Goffey, G., Gluyas, J.G. (Eds.), United Kingdom Oil and Gas

- Fields: 50th Anniversary Commemorative Volume. Geological Society of London Memoirs, **52**, 62–73. <http://dx.doi.org/10.1144/m52-2017-29>.
- Häring, M.O., Schanz, U., Ladner, F. & Dyer, B.C. (2008). Characterisation of the Basel 1 enhanced geothermal system. *Geothermics*, **37**, 469–495. <https://doi.org/10.1016/j.geothermics.2008.06.002>.
- Healy, D. & Hicks, S.P. (2022). De-risking the energy transition by quantifying the uncertainties in fault stability. *Solid Earth* **13**, 15–39. <https://doi.org/10.5194/se-13-15-2022>.
- Heidbach, O., M. Rajabi, X. Cui, K. Fuchs, B. Müller, J. Reinecker, K. Reiter, M. Tingay, F. Wenzel, F. Xie, M. O. Ziegler, M.-L. Zoback, and M. D. Zoback (2018): The World Stress Map database release 2016: Crustal stress pattern across scales. *Tectonophysics*, **744**, 484–498, <https://doi.org/10.1016/j.tecto.2018.07.007>.
- Hennings, P., Dvory, N., Horne, E., Li, P. Savvaidis, A. & Zoback, M. (2021). Stability of the Fault Systems That Host-Induced Earthquakes in the Delaware Basin of West Texas and Southeast New Mexico. *The Seismic Record*, **1** (2), 96–106. <https://doi.org/10.1785/0320210020>.
- Hennissen, J.A.I., Hough, E., Vane, C.H., Leng, M.J., Kemp, S.J. & Stephenson, M.H. (2017). The prospectivity of a potential shale gas play: An example from the southern Pennine Basin (central England, UK). *Marine and Petroleum Geology*, **86**, 1047–1066. <http://dx.doi.org/10.1016/j.marpetgeo.2017.06.033>.
- Hirschberg, S., Wiemer, S., Burgherr, P., 2015. Energy from the Earth. Deep Geothermal as Resource for the Future?, TA-SWISS, 524pp. <http://dx.doi.org/10.3218/3655-8>.
- Holland, A. (2013). Earthquakes triggered by hydraulic fracturing in South-Central Oklahoma. *Bulletin of the Seismological Society of America*, **103** (3), 1784–1792. <https://doi.org/10.1785/0120120109>.
- Hubbert, M.K. & Rubey, W.W. (1959). Role of fluid pressure in mechanics of overthrust faulting: I Mechanics of fluid-filled porous solids and its application to overthrust faulting. *GSA Bulletin*, **70**(2), 115–166. [https://doi.org/10.1130/0016-7606\(1959\)70\[115:ROFPIM\]2.0.CO;2](https://doi.org/10.1130/0016-7606(1959)70[115:ROFPIM]2.0.CO;2).
- Huenges, E., (2016). 25 - Enhanced geothermal systems: Review and status of research and development, in: DiPippo, R. (Ed.), *Geothermal Power Generation*. Woodhead Publishing, pp. 743–761. <https://doi.org/10.1016/B978-0-08-100337-4.00025-5>.
- Hughes, F, Harrison, D, Haarhoff, M, Howlett, P, Pearson, A, Ware, D, Taylor, C, Emms, G & Mortimer, A. (2016). The unconventional Carboniferous reservoirs of the Greater Kirby Misperton gas field and their potential: North Yorkshire's sleeping giant. Geological Society, London, *Petroleum Geology Conference series*, **8**, 611–625, 29 September 2016, <https://doi.org/10.1144/PGC8.5>.
- Jordan, T. H., Y. Chen, P. Gasparini, et al., (2011). Operational earthquake forecasting: State of knowledge and guidelines for utilization, *Annals Geophysics*, **54**, 4, 77 pp. <https://doi.org/10.4401/ag-5350>.
- Kendall, J.M., Butcher, A., Stork, A., Verdon, J., Luckett, R. & Baptie, B., 2019. How big is a small earthquake? Challenges in determining microseismic magnitudes. *First Break*, **37**, 51–56. <https://doi.org/10.3997/1365-2397.n0015>.
- Keranen, K.M. & Weingarten, M. (2018). Induced Seismicity. *Annual Review of Earth and Planetary Sciences*, **46** (1), 149–174.
- Kettlety, T., Verdon, J. P., Werner, M. J., & Kendall, J. M. (2019). Stress transfer from opening hydraulic fractures controls the distribution of induced seismicity. *Journal of Geophysical Research: Solid Earth*, **125**, e2019JB018794. <https://doi.org/10.1029/2019JB018794>
- Kettlety, T., Verdon, J.P, Butcher, A., Hampson, M. & Craddock, L. (2020) High-Resolution Imaging of the ML 2.9 August 2019 Earthquake in Lancashire, United Kingdom, Induced by Hydraulic Fracturing during Preston New Road PNR-2 Operations. *Seismological Research Letters*, **92**(1), 151–169. <https://doi.org/10.1785/0220200187>.

- Kettlety, T. & Verdon, J.P. (2021). Fault Triggering Mechanisms for Hydraulic Fracturing-Induced Seismicity From the Preston New Road, UK Case Study. *Frontiers in Earth Science*, **9**, 670771. <https://doi.org/10.3389/feart.2021.670771> .
- Kettlety, T. & Butcher, A. (2022). Local and moment magnitudes of Preston New Road seismicity, 2018-2019. Local and moment magnitudes of Preston New Road seismicity, 2018-2019. (Dataset). <https://doi.org/10.5285/709cbc2f-af5c-4d09-a4ea-6deb5aa8c5d8>.
- Kovach, R.L. (1974). Source mechanisms for Wilmington Oil Field, California, subsidence earthquakes. *Bulletin of the Seismological Society of America*, **64**, 699–711. <https://doi.org/10.1785/bssa0643-10699>.
- Kozłowska, M., Brudzinski, M. R., Friberg, P., Skoumal, R. J., Baxter, N. D., & Currie, B. S. (2018). Maturity of nearby faults influences seismic hazard from hydraulic fracturing. *Proceedings of the National Academy of Sciences*, **115**(8), E1720–E1729. <https://doi.org/10.1073/pnas.1715284115>
- Kozłowska, M., Jamroz, M. & Olszewska, D. (2021). On the aftershock productivity in mining-induced seismicity—insight into seismicity of Rudna copper ore mine, Poland. *Geophysical Journal International*, **225**(2), 1258–1270. <https://doi.org/10.1093/gji/ggaa613>
- Kwiatek, G., Saarno, T., Ader, T., Bluemle, F., Bohnhoff, M., Chendorain, M., Dresen, G., Heikkinen, P., Kukkonen, I., Leary, P., Leonhardt, M., Malin, P., Martínez-Garzón, P., Passmore, K., Passmore, P., Valenzuela, S. & Wollin, C. (2019). Controlling fluid-induced seismicity during a 6.1-km-deep geothermal stimulation in Finland. *Science Advances*, **5**, eaav7224. <https://doi.org/10.1126/sciadv.aav7224>.
- Langenbruch, C. & Zoback, M.D. (2016). How will induced seismicity in Oklahoma respond to decreased saltwater injection rates? *Science Advances*, **2**, 11, <http://doi.org/10.1126/sciadv.1601542>.
- Langenbruch, C., Weingarten, M. & Zoback, M.D. (2018). Physics-based forecasting of man-made earthquake hazards in Oklahoma and Kansas. *Nature Communications*, **9**, 3946. <https://doi.org/10.1038/s41467-018-06167-4>.
- Lee, K.K., Ellsworth, W.L., Giardini, D., Townend, J., Ge, S., Shimamoto, T., Yeo, I.-W., Kang, T.-S., Rhie, J., Sheen, D.-H., Chang, C., Woo, J.-U. & Langenbruch C. (2019). Managing injection-induced seismic risks. *Science*, **364**(6442), 730–732.
- Lei, X., Huang, D., Su, J, Jiang, G, Wang, X., Wang, H., Guo, X. & Fu H. (2017). Fault reactivation and earthquakes with magnitudes of up to Mw4.7 induced by shale-gas hydraulic fracturing in Sichuan Basin, China. *Nature Scientific Reports*, **7**, 7971. <https://doi.org/10.1038/s41598-017-08557-y>
- Lei, X., Wang, Z. & Su, J. (2019). The December 2018 ML 5.7 and January 2019 ML 5.3 Earthquakes in South Sichuan Basin Induced by Shale Gas Hydraulic Fracturing. *Seismological Research Letters*, **90** (3), 1099–1110. <https://doi.org/10.1785/0220190029>.
- Llenos, A.L. & Michael, A.J. (2013). Modeling Earthquake Rate Changes in Oklahoma and Arkansas: Possible Signatures of Induced Seismicity. *Bulletin of the Seismological Society of America*, **103** (5), 2850–2861. <https://doi.org/10.1785/0120130017>.
- Lund Snee, J.E. & Zoback, M.D. (2020). Multiscale variations of the crustal stress field throughout North America. *Nature Communications*, **11**, 1951. <https://doi.org/10.1038/s41467-020-15841-5>.
- Lund Snee, J.-E. & Zoback, M.D. (2022). State of stress in areas of active unconventional oil and gas development in North America. *AAPG Bulletin* <https://doi.org/10.1306/08102120151>.
- Ma, J., Dineva, S., Cesca, S. & Heimann, S. (2018). Moment tensor inversion with three-dimensional sensor configuration of mining induced seismicity (Kiruna mine, Sweden). *Geophysical Journal International* **213**, 2147–2160. <https://doi.org/10.1093/gji/ggy115>.
- Majer, E.L., Baria, R., Stark, M., Oates, S., Bommer, J., Smith, B. & Asanuma, H. (2007). Induced seismicity associated with Enhanced Geothermal Systems. *Geothermics* **36**, 185–222. <https://doi.org/10.1016/j.geothermics.2007.03.003>.

- Mancini, S., Werner, M.J., Segou, M. & Baptie, B. (2021). Probabilistic Forecasting of Hydraulic Fracturing-Induced Seismicity Using an Injection-Rate Driven ETAS Model. *Seismological Research Letters*, **92**(6), 3471–3481. <https://doi.org/10.1785/0220200454>.
- McGarr, A. (2014). Maximum magnitude earthquakes induced by fluid injection. *Journal of Geophysical Research*, **119**, 1008–1019. <https://doi.org/10.1002/2013JB010597>.
- Megies, T. & Wassermann, J. (2014). Microseismicity observed at a non-pressure-stimulated geothermal power plant. *Geothermics* **52**, 36–49. <https://doi.org/10.1016/j.geothermics.2014.01.002>.
- Meng, L., McGarr, A., Zhou, L., & Zang, Y. (2019). An investigation of seismicity induced by hydraulic fracturing in the Sichuan basin of China based on data from a temporary seismic network. *Bulletin of the Seismological Society of America*, **109**(1), 348–357. <https://doi.org/10.1785/0120180310>
- Mignan, A., Broccardo, M., Wiemer, S. & Giardini, D. (2017). Induced seismicity closed-form traffic light system for actuarial decision-making during deep fluid injections. *Nature Scientific Reports*, **7**, 13607.
- Morris, A., Ferril, D.A. & Henderson, D.B. (1996). Slip-tendency analysis and fault reactivation *Geology* **24**, 275–278. [https://doi.org/10.1130/0091-7613\(1996\)024](https://doi.org/10.1130/0091-7613(1996)024).
- Mousavi, S.M., Ellsworth, W.L., Zhu, W. et al. (2020). Earthquake transformer—an attentive deep-learning model for simultaneous earthquake detection and phase picking. *Nature Communications* **11**, 3952. <https://doi.org/10.1038/s41467-020-17591-w>.
- Nantanoi, S., Rodríguez-Pradilla, G., Verdon, J. (2022). 3D seismic interpretation and fault slip potential analysis from hydraulic fracturing in the Bowland Shale, UK. *Petroleum Geoscience* **28**, 2021–2057. <https://doi.org/10.1144/petgeo2021-057>.
- Naylor, M., Greenhough, J., McCloskey, J., Bell, A. & Main, I. (2009). Statistical evaluation of characteristic earthquakes in the frequency-magnitude distribution of Sumatra and other subduction zone regions. *Geophysical Research Letters*, **36**, L20303. <https://doi.org/10.1029/2009GL040460>.
- Oil and Gas Authority, 2019. Summary report of the scientific analysis of the data gathered from Cuadrilla’s PNR2 hydraulic fracturing operations at Preston New Road, 12pp. <https://www.nstauthority.co.uk/media/6970/oga-summary-of-pnr2-studies-final.pdf>. (accessed 13/06/2022).
- Ogata, Y., (1988). Statistical Models for Earthquake Occurrences and Residual Analysis for Point Processes. *Journal of the American Statistical Association*, **83**, 9–27. <https://doi.org/10.2307/2288914>.
- Ottmøller, L. (2005). The 7 May 2001 induced seismic event in the Ekofisk oil field, North Sea. *Journal of Geophysical Research*, **110**, B10301, <https://doi.org/10.1029/2004jb003374>.
- Palci, F., Fraser, A. J., Neumaier, M., Goode, T., Parkin, K. & Wilson, T. (2020). Shale oil and gas resource evaluation through 3D basin and petroleum systems modelling: a case study from the East Midlands, onshore UK. *Petroleum Geoscience*, **26**(4), 525–543. <https://doi.org/10.1144/petgeo2019-069>.
- Palci, F., Neumaier, M. & Fraser, A. J. (2019). Uplift and Erosion Onshore UK-Implications For Shale Oil and Gas Potential, AAPG Hedberg Conference, AAPG Hedberg Conference, The Evolution of Petroleum Systems Analysis, Houston, Texas.
- Park, Y., Mousavi, S. M., Zhu, W., Ellsworth, W. L., & Beroza, G. C. (2020). Machine learning-based analysis of the Guy-Greenbrier, Arkansas earthquakes: A tale of two sequences. *Geophysical Research Letters*, **47**, e2020GL087032. <https://doi.org/10.1029/2020GL087032>.
- Park, Y., Beroza, G. & Ellsworth, W. (2022). A Deep Earthquake Catalog for Oklahoma and Southern Kansas Reveals Extensive Basement Fault Networks, submitted to *Geophysical Research Letters*, preprint available at <https://doi.org/10.1002/essoar.10508504.1>.

- Parsons, T., Segou, M. & Marzocchi, W. (2014). The global aftershock zone. *Tectonophysics*, **618**, 1–34. <https://doi.org/10.1016/j.tecto.2014.01.038>.
- Petersen, M.D., Mueller, C.S., Moschetti, M.P., Hoover, S.M., Llenos, A.L., et al., (2016). Seismic-Hazard Forecast for 2016 Including Induced and Natural Earthquakes in the Central and Eastern United States. *Seismological Research Letters*, **87**(6), 1327–1341. <https://doi.org/10.1785/0220160072>.
- Pharaoh, T., Haslam, R., Hough, E., Kirk, K., Leslie, G., Schofield, D., Heafford, A., 2020. The Môn–Deemster–Ribblesdale fold–thrust belt, central UK: a concealed Variscan inversion belt located on weak Caledonian crust, in: Hammerstein, J.A., Di Cuia, R., Cottam, M.A., Zamora, G., Butler, R.W.H. (Eds.), *Fold and Thrust Belts: Structural Style, Evolution and Exploration*. *Geological Society of London*, **490**, 153–176. <https://doi.org/10.1144/SP490-2018-109>.
- Pollastro, R.M., Hill, R.J., Jarvie, D.M., Mitchell, H.E., 2003. Assessing Undiscovered Resources of the Barnett–Paleozoic Total Petroleum System, Bend Arch–Fort Worth Basin Province, Texas. AAPG Search and Discovery Article, 17. <https://doi.org/10.1306/10300606008>.
- Pratt, W.E. & Johnson, D.W., 1926. Local Subsidence of the Goose Creek Oil Field. *The Journal of Geology*, **34**, 577–590. <https://doi.org/10.1086/623352>.
- Redmayne, D.W. (1988). Mining induced seismicity in UK coalfields identified on the BGS National Seismograph Network. Geological Society, London, *Engineering Geology Special Publications*, **5**, 405. <https://doi.org/10.1144/GSL.ENG.1988.005.01.45>.
- Redmayne, D.W., Richards, J.A. & Wild, P.W. (1998). Mining-induced earthquakes monitored during pit closure in the Midlothian Coalfield. *Quarterly Journal of Engineering Geology and Hydrogeology*, **31**, 21. <https://doi.org/10.1144/GSL.QJEG.1998.031.P1.03>.
- Richter, C.F. (1935). An instrumental earthquake magnitude scale*. *Bulletin of the Seismological of America*, **25**, 1–32. <https://doi.org/10.1785/bssa0250010001>.
- Roy, C., Nowacki, A., Zhang, X., Curtis, A. & Baptie, B. (2021). Accounting for Natural Uncertainty Within Monitoring Systems for Induced Seismicity Based on Earthquake Magnitudes. *Frontiers in Earth Science*, **9**, article 634688. <https://doi.org/10.3389/feart.2021.634688>.
- Rubinstein, J.L. & Mahani, A.B. (2015). Myths and facts on wastewater injection, hydraulic fracturing, enhanced oil recovery, and induced seismicity. *Seismological Research Letters*, **86**(4), 1060–1067.
- Rubinstein, J.L., Barbour, A.J. & Norbeck, J.H. (2021). Forecasting Induced Earthquake Hazard Using a Hydromechanical Earthquake Nucleation Model. *Seismological Research Letters*, **92** (4): 2206–2220. <https://doi.org/10.1785/0220200215>.
- Schultz, R., Stern, V., Novakovic, M., Atkinson, G. & Gu, Y.G. (2015). Hydraulic fracturing and the Crooked Lake Sequences: Insights gleaned from regional seismic networks. *Geophysical Research Letters*, **42**, 2750–2758.
- Schultz, R., Wang, R., Gu, Y. J., Haug, K. & Atkinson, G. (2017). A seismological overview of the induced earthquakes in the Duvernay play near Fox Creek, Alberta. *Journal of Geophysical Research*, **122**, 492–505.
- Schultz, R., Atkinson, G., Eaton, D. W., Gu, Y. J., & Kao, H. (2018). Hydraulic fracturing volume is associated with induced earthquake productivity in the Duvernay play. *Science*, **359**(6373), 304–308. <https://doi.org/10.1126/science.aao0159>.
- Schultz, R., Skoumal, R. J., Brudzinski, M. R., Eaton, D., Baptie, B., & Ellsworth, W. (2020a). Hydraulic Fracturing-Induced Seismicity. *Reviews of Geophysics*, **58**(3), e2019RG000695 <https://doi.org/10.1029/2019RG000695>.
- Schultz, R., & Wang, R. (2020). A newly emerging case of hydraulic fracturing induced seismicity in the Duvernay East Shale Basin. *Tectonophysics*, **779**, 228393. <https://doi.org/10.1016/j.tecto.2020.228393>.

- Schultz, R., G. Beroza, W. Ellsworth, and J. Baker (2020b). Risk- Informed Recommendations for Managing Hydraulic Fracturing–Induced Seismicity via Traffic Light Protocols, *Bulletin of the Seismological of America*, **110**, 2411–2422, <http://doi.org/10.1785/0120200016>.
- Schultz, R., Beroza, G. C., & Ellsworth, W. L. (2021). A strategy for choosing red-light thresholds to manage hydraulic fracturing induced seismicity in North America. *Journal of Geophysical Research: Solid Earth*, **126**, e2021JB022340. <https://doi.org/10.1029/2021JB022340>
- Schultz, R., Beroza, G. & Ellsworth W. (2021). A risk-based approach for managing hydraulic fracturing–induced seismicity. *Science*, **372**(6541), 504–507. <https://doi.org/10.1126/science.abg5451>
- Schultz, R., Ellsworth, W.L. & Beroza, G.C. Statistical bounds on how induced seismicity stops. *Scientific Reports* **12**, 1184 (2022). <https://doi.org/10.1038/s41598-022-05216-9>.
- Segou, M. & Parsons, T. (2020). A New Technique to Calculate Earthquake Stress Transfer and to Probe the Physics of Aftershocks. *Bulletin of the Seismological Society of America*, **110** (2), 863–873. <https://doi.org/10.1785/0120190033>.
- Shapiro, S. A., Dinske, C., Langenbruch, C. & Wenzel, F. (2010). Seismogenic index and magnitude probability of earthquakes induced during reservoir fluid stimulations. *The Leading Edge*, **29**, 304–309.
- Shapiro, S.A. (2018). Seismogenic Index of Underground Fluid Injections and Productions. *Journal of Geophysical Research: Solid Earth* **123**, 7983-7997. <https://doi.org/10.1029/2018jb015850>.
- Shen, L. W., Schmitt, D. R., & Schultz, R. (2019). Frictional stabilities on induced earthquake fault planes at Fox Creek, Alberta: A pore fluid pressure dilemma. *Geophysical Research Letters*, **46**, 8753–8762. <https://doi.org/10.1029/2019GL083566>.
- Shemeta, J. E., Brooks, C. E., & Lord, C. C. (2019). Well stimulation seismicity in Oklahoma: Cataloging earthquakes related to hydraulic fracturing. In *Unconventional Resources Technology Conference (URTEC)*, (95–106). Brisbane, Australia: Society for Exploration Geophysicists.
- Sheng, Y., Pepin, K.S., & Ellsworth, W.L. (2022). On the Depth of Earthquakes in the Delaware Basin: A Case Study along the Reeves–Pecos County Line. *The Seismic Record*, **2**(1), 29–37.
- Sibson, R. H. (2020). Dual-driven fault failure in the lower seismogenic zone. *Bulletin of the Seismological Society of America*, 110. <https://doi.org/10.1785/0120190190>.
- Silva, V., Crowley, H., Pagani, M., Monelli, D., Pinho, R. (2014). Development of the OpenQuake engine, the Global Earthquake Model’s open-source software for seismic risk assessment, *Natural Hazards*, **72** (3), 1409–1427.
- Skoumal, R.J., Brudzinski, M.R. & Currie, B.S. (2015a). Earthquakes induced by hydraulic fracturing in Poland Township, Ohio. *Bulletin of the Seismological Society of America*, **105**(1), 189–197.
- Skoumal, R.J., Brudzinski, M.R., & Currie, B.S. (2015b). Distinguishing induced seismicity from natural seismicity in Ohio: Demonstrating the utility of waveform template matching. *Journal of Geophysical Research: Solid Earth*, **120**, 6284–6296. <https://doi.org/10.1002/2015JB012265>
- Skoumal, R.J., Ries, R., Brudzinski, M.R., Barbour, A.J., & Currie, B.S. (2018a). Earthquakes induced by hydraulic fracturing are pervasive in Oklahoma. *Journal of Geophysical Research: Solid Earth*, **123**, 10,918–10,935. <https://doi.org/10.1029/2018JB016790>.
- Skoumal, R. J., Brudzinski, M. R., & Currie, B. S. (2018b). Proximity of Precambrian basement affects the likelihood of induced seismicity in the Appalachian, Illinois, and Williston Basins, central and eastern United States. *Geosphere*, **14**(3), 1365–1379.
- Skoumal, R.J., Barbour, A.J., Brudzinski, M.R., Langenkamp, T., & Kaven, J.O. (2020). Induced seismicity in the Delaware Basin, Texas. *Journal of Geophysical Research: Solid Earth*, **125**, e2019JB018558. <https://doi.org/10.1029/2019JB018558>.

- Stephenson, M.H., Angiolini, L., Cozar, P., Jadoul, F., Leng, M.J., Millward, D. & Chenery, S., 2010. Northern England Serpukhovian (early Namurian) farfield responses to southern hemisphere glaciation. *Journal of the Geological Society*, **167**, 1171–1184.
- Suckale, J., (2009). Chapter 2 - Induced Seismicity in Hydrocarbon Fields, *Advances in Geophysics*. Elsevier, pp. 55–106. [https://doi.org/10.1016/S0065-2687\(09\)05107-3](https://doi.org/10.1016/S0065-2687(09)05107-3).
- Suckale, J., (2010). Moderate-to-large seismicity induced by hydrocarbon production. *The Leading Edge*, **29**, 310–319. <https://doi.org/10.1190/1.3353728>.
- Tan, Y.J., Waldhauser, F., Ellsworth, W.L., Zhang, M., Zhu, W., Michele, M., Chiaraluce, L., Beroza, G.C. & Segou, M. (2021). Machine-Learning-Based High-Resolution Earthquake Catalog Reveals How Complex Fault Structures Were Activated during the 2016–2017 Central Italy Sequence. *The Seismic Record*, **1**(1), 11–19. <https://doi.org/10.1785/0320210001>.
- Utsu, T. (1961). A statistical study on the occurrence of aftershocks. *The Geophysical Magazine*, **30**, 521–605.
- Van der Elst, N. J., Page, M. T., Weiser, D. A., Goebel, T. H., & Hosseini, S. M. (2016). Induced earthquake magnitudes are as large as (statistically) expected. *Journal of Geophysical Research: Solid Earth*, **121**, 4575–4590. <https://doi.org/10.1002/2016JB012818>
- Van Eijs, R.M.H.E., Mulders, F.M.M., Nepveu, M., Kenter, C.J. & Scheffers, B.C. (2006). Correlation between hydrocarbon reservoir properties and induced seismicity in the Netherlands. *Engineering Geology*, **84**, 99–111. <https://doi.org/10.1016/j.enggeo.2006.01.002>.
- Van Thienen-Visser, K. & Breunese, J.N. (2015). Induced seismicity of the Groningen gas field: history and recent developments. *The Leading Edge, special section: Injection-induced seismicity*, 664–671.
- Verdon, J. P. & Budge, J. (2018). Examining the capability of statistical models to mitigate induced seismicity during hydraulic fracturing of shale gas reservoirs. *Bulletin of the Seismological Society of America*, **108**, 690–701.
- Verdon, J.P. & Bommer, J.J. (2021). Green, yellow, red, or out of the blue? An assessment of Traffic Light Schemes to mitigate the impact of hydraulic fracturing-induced seismicity. *Journal of Seismology*, **25**, 301–326. <https://doi.org/10.1007/s10950-020-09966-9>.
- Walsh, F.R. III & Zoback, M.D. (2016). Probabilistic assessment of potential fault slip related to injection-induced earthquakes: Application to north-central Oklahoma, USA. *Geology*, **44**(12), 991–994. <https://doi.org/10.1130/G38275.1>.
- Wang, S., Jiang, G., Lei, X., Barbour, A. J., Tan, X., Xu, C., & Xu, X. (2022). Three $M_w \geq 4.7$ earthquakes within the Changning (China) shale gas field ruptured shallow faults intersecting with hydraulic fracturing wells. *Journal of Geophysical Research: Solid Earth*, **127**, e2021JB022946. <https://doi.org/10.1029/2021JB022946>.
- Waters, C.N., Waters, R. A., Barclay, W. J., & Davies, J. R. (2009). A Lithostratigraphical Framework for the Carboniferous Successions of Southern Great Britain (Onshore). British Geological Survey Research Report. RR/09/01. 194pp.
- Waters, C. N., Vane, C. H., Kemp, S. J., Haslam, R. B., Hough, E & Moss-Hayes, V. L. (2019). Lithological and chemostratigraphic discrimination of facies within the Bowland Shale Formation within the Craven and Edale basins, UK. *Petroleum Geoscience*, **26**(2), 325–345.
- Williams, J. D., Fellgett, M. W., & Quinn, M. F. (2016). Carbon dioxide storage in the Captain Sandstone aquifer: determination of in situ stresses and fault-stability analysis, *Petroleum Geoscience*, **22**, 211–222.
- Wilson, M.P., Foulger, G.R., Gluyas, J.G., Davies, R.J. & Julian, B. R. (2017). HiQuake: The Human-Induced Earthquake Database. *Seismological Research Letters*, **88** (6). 1560–1565.
- Yu, H., Harrington, R. M., Liu, Y., & Wang, B. (2019). Induced seismicity driven by fluid diffusion revealed by a near-field hydraulic stimulation monitoring array in the Montney Basin, British Columbia. *Journal of Geophysical Research: Solid Earth*, **124**, 4694–4709.

Appendix 1: Unconventional hydrocarbon resource and exploration in the UK

Shale rocks that may be prospective for oil and gas have been identified from the Carboniferous under large areas of northern England and the Midland Valley of Scotland, and the Jurassic in the Weald and Wessex basins in southern England.

Several studies indicate that the amount of gas likely present in the Carboniferous Bowland Shale Formation may be significantly lower and spatially more restricted than initially estimated by Andrews. (2013) (e.g., Whitelaw et al., 2019; Sims et al., 2021). Work by Hennissen et al (2017) indicates that large areas of shales in the Edale Basin and Widmerpool Gulf, in the midlands, are likely immature for gas and therefore it is unlikely that these areas would be prioritised for gas exploration. The kerogen in the Bowland Shale Formation in parts of the Bowland Basin are described as mixed, including type III but also type I/II (Hampson et al., 2020); in the Cleveland Basin, kerogens are considered type III (Hughes et al., 2016); this has affected the amount of oil and gas that has been generated from the shale.

The development and retention of overpressure in shales is relevant to prospectivity and petrophysical behaviour and has been identified in parts of the Bowland Basin (Clarke et al, 2018) and modelled (but not conclusively proven in the field) in the Gainsborough Trough and the Jurassic Kimmeridge Clay and Oxford Clays formations in the Weald Basin (Palci et al., 2019; 2020). The development of overpressure may be associated with natural fracture networks, perhaps reducing the requirement for extensive hydraulic fracturing and improving the commercial appeal of these areas. The retention of high in-situ overpressure has been suggested as a controlling influence on HFIS (Eaton and Schultz, 2018; Sibson, 2020)

The Cleveland Basin shales are described as a “major unconventional hydrocarbon play”, comprising tight, naturally fractured sandstones interbedded with mudstones, and in contrast to the Bowland area, with only few thin beds of limestone (Hughes et al., 2016). Although the Cleveland Basin shales have undergone multiple phases of burial and uplift, the key horizons have been identified from 3D seismic data with a “high degree of confidence” (Hughes et al., 2016). Collectively, this results in some areas, including the Bowland, Gainsborough and Cleveland basins, remaining exploration targets in terms of resource, whilst other areas may appear less attractive.

The Jurassic shales in the Wessex and Weald basins are clay rich and over large areas have not reached the gas window (Andrews, 2014; Greenhalgh, 2016). Parts of these basins are targets for oil and gas exploration and production, but due to lack of maturity, these shales are unlikely to represent a major interest for shale gas exploration.

Intensive data acquisition occurred in several geographical areas over the last decade See also Figure 4:

- *Fylde, Lancashire.* Cuadrilla Resources drilled the Preese Hall 1 well in November 2011. The Bowland-12 3D seismic survey was acquired in 2012, and 2012 and was used to plan the drilling of further boreholes (Grange Hill 1 and 1Z and Beconshall 1/1Z in 2011, and Anna’s Road 1 in 2012). In 2017-2018, the PNR 1 well was drilled, along with PNR-1z and PNR-2. Summaries and interpretations of these exploration data are given in Clarke et al., (2014; 2018 and 2019); Fellgett et al., (2018); Hampson et al., (2020); Anderson and Underhill., (2020); Anderson et al., (2022) and Nantanoi et al., (2022).
- *North Cheshire.* In 2014, IGas drilled the Ellesmere Port 1 well and acquired the North Dee-15 3D seismic survey in 2015. The well was not hydraulically fractured. These exploration data have not been published in a peer-reviewed paper.
- *North Nottinghamshire.* The Tinker Lane 1 well was drilled by Dart Energy in 2018. IGas acquired the Gainsborough-14 3D survey in 2014, and 2014 and drilled the Springs Road 1 well in and 2019. A summary of these exploration data are given in Palci et al., (2020).
- *North Yorkshire.* Although classified as a conventional exploration well by North Sea Transition Authority (NSTA), Kirby Misperton 8 (drilled in 2013) gives information

regarding the unconventional oil and gas potential in the Cleveland Basin (e.g., Hughes et al., 2016).

- *Formby, Lancashire*. Aurora Resources acquired the Formby-16 3D survey in 2016. These exploration data have not been published in a peer-reviewed paper